

Global analytical potential hypersurfaces for large amplitude nuclear motion and reactions in methane. I. Formulation of the potentials and adjustment of parameters to ab initio data and experimental constraints

Roberto Marquardt and Martin Quack

Citation: *J. Chem. Phys.* **109**, 10628 (1998); doi: 10.1063/1.476513

View online: <http://dx.doi.org/10.1063/1.476513>

View Table of Contents: <http://jcp.aip.org/resource/1/JCPSA6/v109/i24>

Published by the [American Institute of Physics](#).

Additional information on *J. Chem. Phys.*

Journal Homepage: <http://jcp.aip.org/>

Journal Information: http://jcp.aip.org/about/about_the_journal

Top downloads: http://jcp.aip.org/features/most_downloaded

Information for Authors: <http://jcp.aip.org/authors>

ADVERTISEMENT

**AIP**Advances

Submit Now

Explore AIP's new open-access journal

- Article-level metrics now available
- Join the conversation! Rate & comment on articles

Global analytical potential hypersurfaces for large amplitude nuclear motion and reactions in methane. I. Formulation of the potentials and adjustment of parameters to *ab initio* data and experimental constraints

Roberto Marquardt^{a)} and Martin Quack

Laboratorium für Physikalische Chemie, ETH-Zürich (Zentrum), 8092 Zürich, Switzerland

(Received 10 April 1998; accepted 25 August 1998)

Analytical representations of the global potential energy surface of XY_n molecules are developed and applied to model the potential surface of methane in the electronic ground state. The generic analytical representation allows for a compact, robust, and flexible description of potentials for XY_n systems irrespective of the specific nature of the atomic interactions. The functions are global in that structures near several minima of the potential hypersurface as well as saddle points and dissociation limits are well described. Clusters of atoms Y_n can be represented as well by this type of function. Care is taken to implement conditions resulting from the symmetric group S_n and to construct positive definite bilinear forms of special functional forms of certain coordinates (such as bond lengths and bond angles), in order to avoid artifacts in exceptional ranges of the potential hypersurface. These special functional forms include intrinsic, symmetry allowed couplings between coordinates such as bending and stretching. We include linear potential terms in bond angle coordinates, which result in effectively quadratic potential terms for highly symmetric structures. True logical multidimensional 01-switching functions $S_{sw}(r)$ of bond lengths r are used to interpolate between limiting ranges in the hypersurface. The particular form $S_{sw}(r) \sim \exp(-(r_{sw}/r)^{n_{sw}})$ allows us to describe the potential as a multipole expansion representation in the limit of large r ($\rightarrow \infty$). In the application to methane, first the representations are fitted to data from high level *ab initio* calculations using multireference configuration interaction techniques. Additional conditions which help to improve the description of experimental data are considered during the fit. Typically, these conditions involve some parameters or parameter groups and refer to the equilibrium geometry and harmonic force field. Other constraints apply to the energies of dissociation channels. We describe the model potentials METPOT 1 to METPOT 4 in the present work.

© 1998 American Institute of Physics. [S0021-9606(98)01045-9]

I. INTRODUCTION

The formulation of reasonably accurate *global* analytical functional forms describing the potential hypersurfaces of polyatomic molecules has been of central importance in reaction kinetics and spectroscopy for some time.¹⁻⁶ Such functions also play a particularly important role in the approaches to deriving short time intramolecular quantum dynamics from high resolution spectroscopy.⁷ In the context of organic chemistry, methane derivatives *CUXYZ* are obvious prototype systems for many spectroscopic and kinetic properties. However, so far hardly any accurate potentials are available even for the simplest molecular examples of this type and it is the aim of the present paper to contribute to filling this gap of our knowledge.

The ground state potential energy surface of the parent compound methane has been studied in numerous experimental and theoretical investigations (the complete, large list of published work cannot be reproduced here). The understanding of parts of the methane potential surface has been in the focus of contributions in the fields of spectroscopy,⁸⁻¹¹ *ab initio* theory,¹²⁻²⁶ and chemical reaction kinetics based on

statistical theories.^{14,27-34} Duchovic, Hase, and Schlegel have developed a semiglobal, analytical representation of the CH_3+H reaction channel in the electronic ground state potential of methane,¹⁴ which has been used, in modified versions,^{33,34} for classical or semiclassical trajectory calculations. A semiempirical, analytical representation considers also the possibility of the $\text{CH}_4 \rightarrow ({}^1A_1)\text{CH}_2+\text{H}_2$ channel for unimolecular decomposition.³⁵ One analytical representation is completely based on a diatomics-in-molecules (DIM) approach,³⁶ also for the description of bending interactions. The important CH-stretching-bending interaction potential and its relation to the recombination and dissociation kinetics of methane have been investigated in detail from the analysis of the overtone spectrum of the CH chromophore in CHD_3 in the framework of variational calculations of the spectroscopic states.¹¹ Extensions of these studies to nine-dimensional representations of the CHD_3 potential surface in normal coordinates have been given by Iung and Leforestier.³⁷⁻³⁹ Other analytical, anharmonic potential surfaces based on polynomial expansions in isotopically invariant internal coordinates have been developed previously.^{12,40,41} Some of these developments have been reformulated recently,⁴² however, without giving adequate reference to previous work.

We may say that the existing analytical model potentials

^{a)}Present address: Instituto de Física, Universidade Federal do Rio Grande do Sul, 91501-970 Porto Alegre, Brazil.

for methane are not truly global representations of the ground state potential surface. Furthermore, these models cannot cover, with sufficient accuracy, the complete set of experimental data available today. Normally, the models are neither sufficiently *flexible*, nor *robust*, which renders *a posteriori* improvements and adjustments to experimental data difficult. We have therefore decided to develop a new analytical representation of the potential hypersurface of methane, giving special consideration to the criteria of globality, flexibility, and robustness. We aim at the derivation of a global analytical model potential, which may be adjusted as a whole to data pertaining to very different parts of the potential surface. For the determination of model parameters, we consider, in a first, raw adjustment procedure, fitting the model potential to a sufficiently large set of high level *ab initio* energy points on the potential surface [the quality of the *ab initio* calculations being at least comparable to multi-reference configuration interaction (MRCI) methods, for large displacements from equilibrium, in order to account for changes of the character of the electronic wave function during a chemical reaction]. In a second step, an empirical refinement of the model potential is achieved by submitting some of the model parameters or parameter groups to additional constraints given by experimental conditions. When these constraints can be formulated as analytical expressions of the parameters involved, they may be used within the formalism of Lagrange multipliers during the nonlinear adjustment procedure. Several examples may be quoted, from the literature, for the successful employment of this and analogous strategies in the determination of potential energy surfaces (Refs. 4, 5, 11, 21, 43–51, and further references therein).

Throughout this work, we consider the potential surface belonging to the “lowest” electronic state of methane (largely the 1A_1 state). For this molecule, electronically excited states seem to be essentially confined to energies near to and above the dissociation threshold of 112 kcal mol $^{-1}$.^{26,52} Some excited states may nevertheless correlate adiabatically with asymptotically lower lying states, such as for the (3B_1)CH $_2$ +H $_2$ reaction channel, which will be also considered in the present work. With this procedure, we are following the idea of representing a truly adiabatic potential surface, including the possibility of intersystem crossing, within the framework of multivalued potential surfaces and adiabatic corrections to the Born–Oppenheimer approximation where these surfaces intersect.² A next step in the theory would be the simultaneous analytical treatment of several of the lower electronic states, which would, however, demand much information that is not presently available.

The paper is organized as follows: In Sec. II, a short account is given of the *ab initio* calculations used. In Sec. III, we develop the analytical representation in a rather generic form. In Sec. IV, we discuss the results of the adjustment procedure. In a subsequent paper,⁵³ we shall discuss some applications to properties of the model potentials for methane (METPOT 1 to METPOT 4), derived in the context of this work, in comparison with other existing representations, which will further emphasize the complexity of the task and the necessity of current efforts in this field.

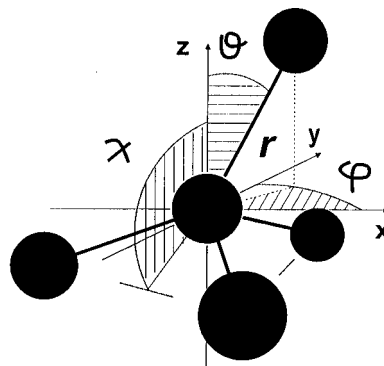


FIG. 1. Definition of internal “angular” coordinates used for the *ab initio* calculation of CH $_4$.

II. AB INITIO CALCULATIONS

The *ab initio* data set used to establish the general shape of the ground state potential surface was initially built up with results from MRD-CI (multireference double excitation-configuration interaction)⁵⁴ calculations reported previously.^{11,15,21} In these calculations, the potential surface was calculated at roughly 600 different nuclear configurations obtained by changing the values of r , ϑ , φ , and χ in Fig. 1. A compilation of the data can be found in Refs. 55 and 56. An additional set of 60 points has been calculated for the purpose of the present work with the aim to sparsely cover the remaining manifolds. However, these points are pivotal of the analytical surface, where the latter yields physically important structures such as saddle points in the multidimensional space. A complete compilation of all points used in the present work will be published separately.⁵⁷

In the calculations, an atomic basis set of double zeta quality was used: for the C atom, Dunning’s contracted [$4s2p$] basis (Ref. 58, Table IIA) with a d -polarization function with exponent 0.75 and contraction coefficient 1.0 (see also Ref. 59, Table II); for each H atom a contracted [$3s$] basis with a p -polarization function was chosen. We reproduce the data used in Table I (from Ref. 56). This results in a total of 40 contracted Gaussian functions. The CI space was calculated with single and double excitations (but frozen core electrons) from reference configurations which were generally different for different nuclear configurations. However, the sum $\sum c_i^2$ over the contribution of the (local) reference configuration to the total electronic wave function was always larger than 0.90 at all geometries. Also, the threshold energy for energy reduction used to test the (local) reference configuration was kept constant at $E_{\text{threshold}} = 5 \times 10^{-6} E_h$ on the whole surface. The final value for the *ab initio* energy used for the fit of the analytical potential surface was obtained with the formula of Langhoff and Davidson⁶⁰ for the estimation of quadruple excitation, in which $\sum c_i^2$ was used, however, instead of the leading reference configuration coefficient c_0^2 .

In the present calculations, the lowest *ab initio* energy is -176.1183 aJ ($-40.39643 E_h$) at $r_e = 1.093$ Å (1 Å = 100 pm, 1 aJ = 10^{-18} J corresponding to 602.21 kJ/mol $^{-1}$). The absolute electronic energy was calculated by Grev and

TABLE I. $[4s2p]+d$ and $[3s]+p$ atomic basis set used in the MRD-CI calculations of CH_4 .^a

Center	Type	Exponent	Coefficient
C	s	4232.61	0.002 029
		634.882	0.015 535
		146.097	0.075 411
		42.497 4	0.257 121
		14.189 2	0.596 555
		1.966 60	0.242 517
	s	5.147 70	1.000 000
	s	0.496 20	1.000 000
	s	0.153 30	1.000 000
	p	18.155 7	0.018 534
		3.986 40	0.115 442
		1.142 93	0.386 206
		0.359 45	0.640 089
	p	0.114 60	1.000 000
d	0.750 00	1.000 000	
H	s	33.640 0	0.025 374
		5.058 00	0.189 684
		1.147 00	0.852 933
	s	0.321 10	1.000 000
	s	0.101 30	1.000 000
	p	1.000 00	1.000 000

^aFrom Ref. 56.

Schaefer with the CCSD(T) method to be -176.574 aJ ($-40.501 E_h$),²² Garmer and Anderson obtain the value (-40.506 ± 0.002) E_h with the quantum Monte Carlo method,⁶¹ and in Ref. 26 the value $-40.516 E_h$ is reported. Probably the best experimental estimate is (-40.526 ± 0.001) E_h ⁶² (in agreement with more recent data⁶³).

Also, in the present calculations, the energy at $r_{\text{CH}} = 3.18 \text{ \AA}$ and relaxed CH_3 frame is 0.737 aJ higher than the energy minimum. This value can be compared with the electronic dissociation energy, and is roughly 0.04 aJ less than the probably most accurate present *ab initio* value $D_e = 0.779$ aJ,^{22,25} obtained with coupled cluster single double (triple) [CCSD(T)] and correlation calculation between all electrons (in Ref. 26 comparable results are derived from single and multiple reference CI calculations). In these calculations, the equilibrium CH bond length was optimized within the CCSD(T) method, and agrees well with results from the analysis of experimental rotational constants.^{10,64} When the anharmonic zero point energy is considered (as in Ref. 65), the resulting dissociation energy is $D_0 = 0.718$ aJ ($432.63 \text{ kJ mol}^{-1}$), which is in good agreement with experimental (thermo and photochemical) data (e.g., $D_0 = 431.8 \text{ kJ mol}^{-1}$).^{63,66} However, errors of up to 1.0 kJ mol^{-1} (0.002 aJ) are possible in the determination of anharmonic zero point energies, as will be discussed in a subsequent paper.⁵³ We have estimated $D_e = 0.7831$ aJ, in the present work, from the experimental data in Ref. 63 and harmonic zero point energy corrections from experimental

force fields.^{10,67} Our estimation from anharmonic zero point energy corrections yields $D_e = 0.7823$ aJ.⁵³

In order to give a global estimation of errors in our *ab initio* calculations, we have compared the experimentally derived potential functions for the CH chromophore in CHD_3 with corresponding potentials from *ab initio* calculations,^{21,68} and tried to determine, from this comparison, a formula for the ‘‘uncertainty’’ of our *ab initio* data as a function of the potential energy. The result of our analysis may be given as

$$\sigma(E)/hc = 10^{0.048[\lg((E-E_{\min})/hc \text{ cm}^{-1})]^{2.74}} \text{ cm}^{-1}. \quad (1)$$

This formula gives a rough estimation of deviations of the theoretical data from expected experimental results on the average (in special cases deviations can even be larger but within the same order of magnitude) and as such will prove to be useful in weighting the *ab initio* data during the adjustment procedure to be described below. A graphical representation of this function is given in Fig. 4 below.

III. RESULTS FOR THE ANALYTICAL REPRESENTATIONS

A. General structure of the functions METPOT 1 to METPOT 4

The potential of a covalently bound molecule of the type XY_n with one central atom X and several valence electrons is best described as a function of the bond lengths $r_i = r(\text{XY}(i))$ ($i = 1, \dots, n$), as already noted by Bjerrum.⁶⁹ r_i is the distance between the nuclei of the atoms X and $Y(i)$, which are considered to be two strongly interacting bodies in a covalently bound molecule, and potential functions of r_i thus describe two-body interactions. Since the complete potential function of methane must be symmetric with respect to permutations of the four identical H atoms, one term of the potential function can be expected to be of the form

$$V_{s(\text{XY})} = \sum_{i=1}^4 f_{s(\text{XY})}(r_i), \quad (2)$$

where $f_{s(\text{XY})}$ is an appropriately chosen bond-stretching potential function to be described below.

Other two-body interactions are described by functions of the $Y(i)-Y(j)$ interatomic distance r_{ij} . In methane, if r_{ij} is close to the equilibrium value, these interactions are likely to be weak compared to the strong interactions of the central force field. However, functions of these coordinates are needed to describe the H-H interaction potentials at large values of the corresponding C-H bond lengths. For the purpose of obtaining a global potential surface, it is helpful to consider such interactions in the region of bound methane, too, which is done, in the present work, with potential functions of the form

$$V_{s(\text{YY})} = \sum_{j=1}^4 \sum_{i>j} f_{s(\text{YY})}(r_{ij}), \quad (3)$$

where $f_{s(\text{YY})}$ is an appropriately chosen stretching potential function to be described below.

The coordinates r_{ij} have been used before to describe the bending potential in CH_4 ,³⁶ which has then been interpreted as arising from two-body interaction terms between the H atoms. However, we found that functions of the valence bond angles α_{ij} , which have been widely used in the literature to describe bending force fields of polyatomic molecules, are also more adequate to describe the global, anharmonic bending potential of methane. Potential functions of valence bond angles describe implicitly three-body interactions between the $Y-X-Y$ atoms.

In the present work, the total potential energy surface for the methane system is given as a sum

$$V = \underbrace{V_{s(XY)} + V_{s(YX)}}_{\text{two-body terms}} + \underbrace{V_{b(YXY)}}_{\text{three-body term}}, \quad (4)$$

where $V_{b(YXY)}$ is a bending potential surface to be described in detail in Sec. III C. It will be a function of the valence bond angles, to a large extent, and will have a somewhat weaker dependence on the bond lengths. Thus, all terms in Eq. (4) will contribute to the harmonic stretching potential of methane close to equilibrium. Since there is also some dependence of $V_{s(YX)}$ on the bending angles, both terms $V_{s(YX)}$ and $V_{b(YXY)}$ will contribute to the harmonic bending potential. For simplicity, we call $V_{s(XY)}$ the ‘‘C–H bond stretching’’ potential, $V_{b(YXY)}$ the ‘‘H–C–H bending’’ potential, and $V_{s(YX)}$ the ‘‘pair’’ potential, in case of methane.

For the purpose of achieving a compact and robust representation of the potential surface, we have chosen to include some dynamical properties directly into specific functions of the coordinates, which will be used to build up the individual potential terms. This approach differs somewhat from the common analytical representation of the potential surface as a many-body expansion of functions of the interatomic distances.² Many-body expansions are usually sums of many terms, which may have positive or negative signs. Such sums are less robust representations in the sense that the global form of the potential may ‘‘fluctuate’’ considerably in those regions of the configuration space, for which there is less information (either from *ab initio* calculations or experimental data), and where it may even become unphysical. On the other hand, analytical representations which use specific coordinate functions may show too high a degree of bias. The present representation is built up of global forms, which were chosen adequately to describe the data from *ab initio* calculations. Within the constraint of using these forms, it is kept as flexible as possible.

B. The C–H bond stretching potential

We use modified Morse coordinates to describe the bond-stretching potential functions $f_{s(XY)}$. Equation (2) becomes:

$$V_{s(XY)} = \frac{1}{2} F_s \sum_{i=1}^4 y_i^2, \quad (5)$$

where

$$y_i = \frac{1 - \exp(-a_s \Delta r_i)}{a_s} \cdot \left(1 + \epsilon_6 \exp\left(-\left(\frac{r_s}{r_i}\right)^6\right) + \epsilon_8 \exp\left(-\left(\frac{r_s}{r_i}\right)^8\right) \right), \quad (6)$$

$$\Delta r_i = r_i - r_i^{\text{eq}}. \quad (7)$$

$y = (1 - \exp(-a\Delta r))/a$ gives rise to the Morse potential⁷⁰ $V(r) \sim y^2$, which has been widely used to describe covalent bond potentials, mostly of diatomic molecules. a_s is the usual exponential parameter of the Morse potential, ϵ_6 , ϵ_8 , and r_s are new, adjustable parameters. It is assumed that possible values of these parameters lie in the intervals $-1 < \epsilon_6$, $\epsilon_8 < 1$, and $r_e \ll r_s$, such that $\exp(-(r_s/r_e)^6)$ will always be much smaller than one. We can thus expect $y_i \approx \Delta r_i$ close to equilibrium. We shall show below, that the equilibrium bond length r_i^{eq} in Eq. (7) should be chosen as a function of the remaining bond lengths r_j ($j \neq i$), in order to achieve full flexibility in the description of the harmonic stretching force field.

With the choice $f_{s(XY)}(r_i) \sim y_i^2$ in Eq. (2) we can describe a parabolic potential in the vicinity of the equilibrium structure, and the asymptotically correct behavior

$$V_{s(XY)} \approx D_e^I - \frac{C^I}{r_i^6}, \quad r_i \rightarrow \infty, \quad (8)$$

$$V_{s(XY)} \approx D_e^{II} - \frac{C^{II}}{r_i^6} - \frac{C^{II}}{r_j^6}, \quad r_i, r_j \rightarrow \infty. \quad (9)$$

D_e^I is the dissociation energy for breaking one, D_e^{II} for breaking two bonds (analogous for breaking further bonds). Specifically,

$$D_e^K = n_K \frac{F_s(n_K)(1 + \epsilon_6(n_K) + \epsilon_8(n_K))^2}{2a_s^2(n_K)}, \quad (10)$$

with $n_I = 1$, $n_{II} = 2$, $n_{III} = 3$, $n_{IV} = 4$. $F_s(1)$ in Eq. (10) means the value of F_s in the methane limit, $F_s(2)$ the value of F_s in the limit of the methyl radical, $F_s(3)$ in the limit of the methylene radical, and so forth with analogous meaning for all the other parameters [$\epsilon_6(n_K)$, $\epsilon_8(n_K)$ and $a_s(n_K)$ in Eq. (10)]. As will be discussed below, all parameters will actually be slowly varying functions of the bond lengths, which will in turn parametrize the different dissociation channels of the originally bound compound. Within this approach, we are using that a dissociation $\text{CH}_n \rightarrow \text{CH}_{n-1} + \text{H}$ occurs whenever a CH bond length becomes large. It will be shown that the potential of the CH_{n-1} product can be correctly described by the same analytical representation derived for the CH_n reactant, provided the parameter values are switched accordingly. Slowly varying functions will be described by appropriate switching functions, such that the corresponding parameters will change very little in the definition range of the specific CH_n aggregate. The properties of the switching functions will be discussed in Sec. III E.

In the definition of y_i in Eq. (6) we have assumed that the r^{-6} -behavior is the leading term at large values of the bond length. More general r^{-1} expansions are possible, though, whenever the requirement is fulfilled that their con-

tribution to the potential function close to equilibrium is negligible. For the present purposes, the two terms r^{-6} and r^{-8} guarantee enough flexibility in the description of the dissociation energy in Eq. (10). It follows that, for methane, the dispersion constant C^1 in Eq. (9) is given by $C^1 = F_s(1)\epsilon_6(1)r_s(1)^6$.

The sum in Eq. (5) is not the most general quadratic expression allowed by symmetry. There are two independent, totally symmetric combinations of quadratic forms involving the bond lengths (or functions thereof). One type is given in Eq. (5), the other being proportional to $\sum_{ij} y_i y_j$. The latter sum could, in principle, lead to large negative contributions to the potential surface and consequently does not fulfill the requirement of a robust representation. In a more robust and flexible approach, used in our previous attempts to describe the potential surface of methane with the models METPOT 1^{64,71,72} and METPOT 2,⁷³ we considered positive definite quadratic forms of symmetrized coordinates

$$V_s = \frac{1}{2}F_{s_1}S_{s_1}^2 + \frac{1}{2}F_{s_2}(S_{s_{2x}}^2 + S_{s_{2y}}^2 + S_{s_{2z}}^2), \quad (11)$$

where

$$S_{s_1} = \frac{1}{2}(y_1^{(1)} + y_2^{(1)} + y_3^{(1)} + y_4^{(1)}), \quad (12)$$

$$S_{s_{2x}} = \frac{1}{2}(y_1^{(2)} - y_2^{(2)} + y_3^{(2)} - y_4^{(2)}), \quad (13)$$

$$S_{s_{2y}} = \frac{1}{2}(y_1^{(2)} - y_2^{(2)} - y_3^{(2)} + y_4^{(2)}), \quad (14)$$

$$S_{s_{2z}} = \frac{1}{2}(y_1^{(2)} + y_2^{(2)} - y_3^{(2)} - y_4^{(2)}). \quad (15)$$

S_{s_1} and S_{s_2} define two possible irreducible representations of the symmetric group S_4 in the space generated by the four bond lengths. In these equations, the modified Morse coordinate was defined as

$$y_i^{(l)} = \frac{1 - \exp(-a_s^{(l)}(r_i - r_e))}{a_s^{(l)}} \cdot \left(1 + \epsilon_6 \exp\left(-\left(\frac{r_s}{r_i}\right)^6\right) + \epsilon_8 \exp\left(-\left(\frac{r_s}{r_i}\right)^8\right) \right), \quad (16)$$

with $l=1$ or 2 and different anharmonicity parameters $a_s^{(1)}$ and $a_s^{(2)}$.

The stretching potential in Eq. (11) is awkward for the treatment of CH_3 and CH_2 in the asymptotic limits of large bond lengths, because these molecules have lower symmetry. On the other hand, the stretching potential proposed in Eq. (5) has a simple physical interpretation as a sum of central force fields, which enables the description of the total energy after partial atomizations $\text{CH}_n \rightarrow \text{CH}_{n-1} + \text{H}$ in an easy way as a sum of $n-1$ central force fields plus a constant energy corresponding to the dissociation energy.

In order to increase the flexibility of the potential function in Eq. (5), we have considered the equilibrium bond length r_i^{eq} in Eq. (7) to be the following function of the remaining bond lengths, which will in fact change the value of the equilibrium bond length as a function of the degree of atomization:

$$\begin{aligned} r_i^{\text{eq}}(r_1, \dots, r_{i-1}, r_{i+1}, \dots, r_4) = & r_e(1) \{S_{q_r}(r_1) \cdots S_{q_r}(r_{i-1}) S_{q_r}(r_{i+1}) \cdots S_{q_r}(r_4)\} \\ & + r_e(2) \{S_{p_r}(r_1) \cdots S_{q_r}(r_{i-1}) S_{q_r}(r_{i+1}) \cdots S_{q_r}(r_4) \\ & \quad + S_{q_r}(r_1) S_{p_r}(r_2) \cdots S_{q_r}(r_{i-1}) S_{q_r}(r_{i+1}) \cdots S_{q_r}(r_4) \\ & \quad \vdots \\ & \quad + S_{q_r}(r_1) \cdots S_{q_r}(r_{i-1}) S_{q_r}(r_{i+1}) \cdots S_{p_r}(r_4)\} \\ & + r_e(3) \{S_{p_r}(r_1) S_{p_r}(r_2) \cdots S_{q_r}(r_{i-1}) S_{q_r}(r_{i+1}) \cdots S_{q_r}(r_4) \\ & \quad \vdots \\ & \quad + S_{q_r}(r_1) \cdots S_{q_r}(r_{i-1}) S_{q_r}(r_{i+1}) \cdots S_{p_r}(r_3) S_{p_r}(r_4)\} \\ & + r_e(4) \{S_{p_r}(r_1) \cdots S_{p_r}(r_{i-1}) S_{p_r}(r_{i+1}) \cdots S_{p_r}(r_4)\}. \end{aligned} \quad (17)$$

The $r_e(k)$ ($k=1, \dots, 4$) are the equilibrium bond lengths of the $\text{CH}_{(5-k)}$ system. S_{p_r} and $S_{q_r} \equiv 1 - S_{p_r}$ are given by the function

$$S_{p_r}(r) = \tanh(a_r(r - r_e)). \quad (18)$$

Here, $a_r > 0$ is needed in order to guarantee the desired asymptotic behavior $S_{q_r}(r \rightarrow \infty) \rightarrow 0$.

r_e in Eq. (18) [as well as in Eq. (16)] is the parameter for the equilibrium bond length, which, like all other surface parameters, is considered to be a slowly varying function of the bond lengths. Near the minimum for CH_n , r_e assumes the value given by $r_e(5-n)$, likewise r_i^{eq} . However, as for all slowly varying functions of the bond lengths, $|(\partial r_e / \partial r_i)_{r_i=r_e}| \ll 1$. In contrast, because $\partial r_i^{\text{eq}} / \partial r_j \propto a_r$, r_i^{eq} is considered to be a rapidly changing function of r_j .

We see that, to first order in $dr_i = r_i - r_e$ one obtains, i.e., in the methane limit, $\Delta r_i = r_i - r_i^{\text{eq}} = dr_i + a_r(1)(r_e(2) - r_e(1))(dr_k + dr_l + dr_m)$, with $i \neq k$, $i \neq l$, $i \neq m$. Thus, close to equilibrium, the force field $V_s \approx \frac{1}{2} F_s \sum \Delta r_i^2$ contains contributions proportional to $a_r(r_i - r_e)(r_j - r_e)$. Consequently, a_r plays the role of the $f_{rr'}$ force constant in the harmonic stretching force field. Equation (18) can be generalized to include polynomials of $(r - r_e)$, which may be useful, e.g., whenever the signs of $f_{rr'}$ and a_r need to be chosen independently, or when higher order cross terms between stretching coordinates need to be considered. Currently, a linear function for the argument in Eq. (18) is sufficient and the condition $a_r > 0$ happens to impose no further restriction on the adequate description of the experimental quadratic force field of methane and subcompounds.

Bond stretching potentials of the kind given in Eq. (5) have been used before (see, e.g., Ref. 2), in particular for methane.^{14,33,34} Stretching potentials as in Eq. (11), defined in symmetrized coordinates, have also been used before, for instance for the representation of the ammonia potential,^{45,74} for H_2CO ,⁷⁵ and methane.^{10,12} However, the specific representations used in these references were either not flexible or not robust enough. The stretching coordinate functions used there [usually $f_{s(XY)}(r_i) \sim (r_i - r_e)^2$] do not describe the anharmonic behavior of the stretching potential sufficiently well, and polynomial forms of higher degrees had to be considered, in addition. Moreover, stretching, bending, and coupling potentials are treated as expansion terms in the same polynomial expansion, which leads to less robust representations. In our first representation of the methane potential (METPOT 1), we also considered explicit interaction potential terms between the stretching and bending manifolds, which we shall describe at the end of Sec. III C. We first present a new way to describe the stretching–bending coupling potential under omission of explicit coupling terms by considering bending potential functions with a strong parametric dependence on the stretching coordinates (bond lengths).

C. The H–C–H bending potential

The Morse potential coordinate y_i is especially useful for the description of compact and robust bond stretching potentials, because it has the intrinsically correct asymptotic behavior at large values of the bond length. A corresponding coordinate choice for the description of global bending potentials is much more difficult. It would be useful for a robust representation of the bending potential to describe it as a quadratic (or positive definite) function of an appropriate bending coordinate, which could equally well serve as a path for large amplitude bending motions, such as the inversion or stereomutation in polyatomic molecules. Normally, this motion involves large changes in many of the valence bond angles. To our knowledge, at present there is no simple coordinate choice for the compact description of the inversion motion of methane.

We have found that expansions involving the cosine of valence bond angles are a better choice than the valence angles. One reason is the better performance in fitting the *ab initio* data. Another reason is that, from geometrical consid-

erations, potential terms pertaining to CH_2 subsystems automatically have the correct saddle point behavior at the linear arrangement. The cosine of the valence angles also leads to a simple description of the out-of-plane bending potential of the methyl radical, which we will discuss below. Expressions using the cosine of valence angles have been used in Refs. 36, 76, and 77.

We introduce here the following expressions:

$$x_{ij}^{(k)} = (\cos(\alpha_{ij}) - c_{ij}^{\text{eq}}(\dots r_k \dots)) y_d^{(k)}(r_i) y_d^{(k)}(r_j). \quad (19)$$

The meaning of (k) will be explained below. The functions $y_d^{(k)}$ are given by

$$y_d^{(k)}(r_i) = \exp\left(-\sum_{l=1}^{l_{\text{max}}} a_{d_l}^{(k)} (\Delta r_i)^l\right), \quad (20)$$

for the models METPOT 1, 3, and 4, and by

$$y_d^{(k)}(r_i) = \exp\left(-\sum_{l=1}^{l_{\text{max}}} \tilde{a}_{d_l}^{(k)} (\Delta r_i)^l\right), \quad (21)$$

for METPOT 2, where $l_{\text{max}} = 3$ in the present work (larger expansions are possible, in principle). Δr_i has been defined in Eq. (7). In order to guarantee the correct asymptotic behavior $y_d^{(k)}(r_i \rightarrow \infty) \rightarrow 0$ (free rotation of the i th H atom after breaking the C–H bond), the highest nonvanishing coefficient $a_{d_l}^{(k)}$ must be positive. The damping effect of large CH bond lengths on the bending potential cannot be interpreted in a simple way from theoretical considerations based upon the structure of the electronic wave function in the Born–Oppenheimer approximation. We have also tried other possible definitions for y_d , such as $y_d(r) \sim (r_e/r)^6$ or with other exponents or polynomials in r^{-1} . The definition given in Eq. (20) yielded the best fits. An exponential damping behavior was found in Refs. 78 and 79, which was discussed in Ref. 78 in connection with a “bond-energy-bond-order” analysis of the bending force field dependence on the stretching potential of triatomic molecules⁸⁰ (see also Ref. 27).

The function $c_{ij}^{\text{eq}}(\dots r_k \dots)$, introduced in Eq. (19), changes the value of the cosine of the equilibrium bond angle depending on the values of the bond lengths, following the same ideas as discussed before for the function r_i^{eq} in Eq. (17). For the potential model METPOT 1 we used the function

$$c_{ij}^{\text{eq}}(r_1, \dots, r_4) = \cos(\alpha_{ij}^{\text{eq}}(r_1, \dots, r_4)), \quad (22)$$

$$\alpha_{ij}^{\text{eq}}(r_1, \dots, r_4) = -3 \arccos\left(-\frac{1}{3}\right) + \arccos(h_i) + \arccos(h_j) + \arccos\left(\frac{3h_k^2 - 1}{2}\right) + \arccos\left(\frac{3h_l^2 - 1}{2}\right), \quad (23)$$

with indices $k \neq l \neq i \neq j$ and

$$h_i = -\frac{1}{3} + \frac{2 \arctan(a_c(r_i - r_e))}{3\pi}. \quad (24)$$

For METPOT 2, 3, and 4 we used

$$c_{ij}^{\text{eq}}(r_k, r_l) = c_e(1) S_{q_c}(r_k) S_{q_c}(r_l) + c_e(2) \{S_{p_c}(r_k) S_{q_c}(r_l) + S_{q_c}(r_k) S_{p_c}(r_l)\} + c_e(3) S_{p_c}(r_k) S_{p_c}(r_l), \quad (25)$$

where

$$S_{p_c}(r_i) = \frac{2}{\pi} \arctan\left(\frac{\pi}{2} a_c(r_i - r_e)\right) \quad (26)$$

for METPOT 2, and

$$S_{p_c}(r_i) = \tanh(a_c(r_i - r_e)) \quad (27)$$

for METPOT 3 and 4 ($S_{q_c}(r_i) \equiv 1 - S_{p_c}(r_i)$).

The function used for METPOT 1 in Eq. (23) yields the values $c_{ij}^{\text{eq}} = -1/3$, if $r_i = r_e(1)$ (for all i), $c_{ij}^{\text{eq}} = -1/2$ for $i, j = 2, 3, 4$, if $r_1 \rightarrow \infty$, and $c_{34}^{\text{eq}} = -0.649\,846$, if $r_1 \rightarrow \infty$ and $r_2 \rightarrow \infty$. Within this model, $c_{ij}^{\text{eq}} = 0$ for $r_1 \rightarrow \infty$ and $j = 2, 3, 4$, similar to the analytical representations in Refs. 14 and 34. Although this is not a serious problem for the description of the potential surface, since changes in $(\cos(\alpha_{ij}) - c_{ij}^{\text{eq}})$ are damped to zero if $r_i \rightarrow \infty$ or $r_j \rightarrow \infty$, the effective use of an equilibrium bond angle in the limit of large neighbor bond lengths remains an unsatisfactory issue, which was finally avoided in the functions used subsequently for METPOT 2, 3, and 4. The equilibrium cosine function in Eq. (25) depends only on two (adjacent) bond lengths and is, in spite of this, more flexible in the determination of the actual equilibrium values at $r_i = r_e$.

The bending potential is set up as a polynomial in the coordinates x_{ij} . In order to guarantee positive definite forms, we introduce symmetry adapted linear combinations of these coordinates. In methane, the x_{ij} span a six-dimensional vector space representation of S_4 (isomorphous to T_d), which can be reduced to one one-dimensional, one two-dimensional and one three-dimensional irreducible representations of this group:

$$S_{b_1}^{(k)} = x_{12}^{(k)} + x_{13}^{(k)} + x_{14}^{(k)} + x_{23}^{(k)} + x_{24}^{(k)} + x_{34}^{(k)}, \quad (28)$$

$$S_{b_{2_a}}^{(k)} = \frac{2(x_{12}^{(k)} + x_{34}^{(k)}) - (x_{13}^{(k)} + x_{24}^{(k)} + x_{14}^{(k)} + x_{23}^{(k)})}{\sqrt{3}}, \quad (29a)$$

$$S_{b_{2_b}}^{(k)} = (x_{13}^{(k)} + x_{24}^{(k)}) - (x_{14}^{(k)} + x_{23}^{(k)}), \quad (29b)$$

$$S_{b_{3_x}}^{(k)} = x_{13}^{(k)} - x_{24}^{(k)}, \quad (30a)$$

$$S_{b_{3_y}}^{(k)} = x_{14}^{(k)} - x_{23}^{(k)}, \quad (30b)$$

$$S_{b_{3_z}}^{(k)} = x_{12}^{(k)} - x_{34}^{(k)}. \quad (30c)$$

The index (k) describes a power ordering which we define now. The bending potential is a *quadratic* form of the following type of coordinates, which will be distinguished from the coordinates in Eq. (28)–(30) by omission of the index (k) :

$$S_{b_n} = S_{b_n}^{(1)} + \sum_{k=2}^{k_{\max}} \sum_{i_1 \dots i_k} a_{b_{i_1 \dots i_k}} S_{b_{i_1}}^{(k)} \dots S_{b_{i_k}}^{(k)}. \quad (31)$$

S_{b_n} has the same transformation properties as $S_{b_n}^{(k)}$. For $k_{\max} = 4$, there are 24 different variables $S_{b_n}^{(k)}$. Due to symmetry conditions, many of the coefficients $a_{b_{i_1 \dots i_k}}$ vanish, or are linearly dependent. In Eqs. (32)–(37), we collect all symmetry allowed combinations yielding a total of 40 independent coefficients for $k_{\max} = 4$.

$$\begin{aligned} S_{b_1} = & S_{b_1}^{(1)} + a_{b_1} S_{b_1}^{(2)^2} + a_{b_2} (S_{b_{2_a}}^{(2)^2} + S_{b_{2_b}}^{(2)^2}) + a_{b_3} (S_{b_{3_z}}^{(2)^2} + S_{b_{3_x}}^{(2)^2} + S_{b_{3_y}}^{(2)^2}) + a_{b_4} S_{b_1}^{(3)^3} + a_{b_5} (S_{b_{2_a}}^{(3)^3} - 3S_{b_{2_a}}^{(3)} S_{b_{2_b}}^{(3)^2}) + a_{b_6} (S_{b_{2_a}}^{(3)} \\ & \times [2S_{b_{3_z}}^{(3)^2} - S_{b_{3_x}}^{(3)^2} - S_{b_{3_y}}^{(3)^2}] + \sqrt{3} S_{b_{2_b}}^{(3)} [S_{b_{3_x}}^{(3)^2} - S_{b_{3_y}}^{(3)^2}]) + a_{b_7} S_{b_{3_z}}^{(3)} S_{b_{3_x}}^{(3)} S_{b_{3_y}}^{(3)} + a_{b_8} S_{b_1}^{(4)^4} + a_{b_9} (S_{b_{2_a}}^{(4)^2} + S_{b_{2_b}}^{(4)^2})^2 + a_{b_{10}} (S_{b_{3_z}}^{(4)^2} + S_{b_{3_x}}^{(4)^2} \\ & + S_{b_{3_y}}^{(4)^2}) (S_{b_{2_a}}^{(4)^2} + S_{b_{2_b}}^{(4)^2}) + a_{b_{11}} \left(\left[S_{b_{3_z}}^{(4)^2} - \frac{S_{b_{3_x}}^{(4)^2} + S_{b_{3_y}}^{(4)^2}}{2} \right] [S_{b_{2_a}}^{(4)^2} - S_{b_{2_b}}^{(4)^2}] - \sqrt{3} S_{b_{2_a}}^{(4)} S_{b_{2_b}}^{(4)} [S_{b_{3_x}}^{(4)^2} - S_{b_{3_y}}^{(4)^2}] \right) + a_{b_{12}} (S_{b_{3_z}}^{(4)^4} + S_{b_{3_x}}^{(4)^4} \\ & + S_{b_{3_y}}^{(4)^4}) + a_{b_{13}} (S_{b_{3_z}}^{(4)^2} S_{b_{3_x}}^{(4)^2} + S_{b_{3_x}}^{(4)^2} S_{b_{3_y}}^{(4)^2} + S_{b_{3_y}}^{(4)^2} S_{b_{3_z}}^{(4)^2}), \end{aligned} \quad (32)$$

$$\begin{aligned} S_{b_{2_a}} = & S_{b_{2_a}}^{(1)} + a_{b_{14}} (S_{b_{2_a}}^{(2)^2} - S_{b_{2_b}}^{(2)^2}) + a_{b_{15}} \left(S_{b_{3_z}}^{(2)^2} - \frac{S_{b_{3_x}}^{(2)^2} + S_{b_{3_y}}^{(2)^2}}{2} \right) + a_{b_{16}} S_{b_{2_a}}^{(3)} (S_{b_{2_a}}^{(3)^2} + S_{b_{2_b}}^{(3)^2}) \\ & + a_{b_{17}} S_{b_{2_a}}^{(3)} (S_{b_{3_z}}^{(3)^2} + S_{b_{3_x}}^{(3)^2} + S_{b_{3_y}}^{(3)^2}) + a_{b_{18}} (S_{b_{2_a}}^{(4)^4} - S_{b_{2_b}}^{(4)^4}) + a_{b_{19}} ([S_{b_{2_a}}^{(4)^2} - S_{b_{2_b}}^{(4)^2}]^2 - 4S_{b_{2_a}}^{(4)^2} S_{b_{2_b}}^{(4)^2}) + a_{b_{20}} (S_{b_{2_a}}^{(4)^2} - S_{b_{2_b}}^{(4)^2}) \\ & \times (S_{b_{3_z}}^{(4)^2} + S_{b_{3_x}}^{(4)^2} + S_{b_{3_y}}^{(4)^2}) + a_{b_{21}} (S_{b_{2_a}}^{(4)^2} + S_{b_{2_b}}^{(4)^2}) \left(S_{b_{3_z}}^{(4)^2} - \frac{S_{b_{3_x}}^{(4)^2} + S_{b_{3_y}}^{(4)^2}}{2} \right) + a_{b_{22}} S_{b_{2_a}}^{(4)} S_{b_{3_z}}^{(4)} S_{b_{3_x}}^{(4)} S_{b_{3_y}}^{(4)} \\ & + a_{b_{23}} (S_{b_{3_x}}^{(4)^2} S_{b_{3_y}}^{(4)^2} - \frac{1}{2} S_{b_{3_z}}^{(4)^2} [S_{b_{3_x}}^{(4)^2} + S_{b_{3_y}}^{(4)^2}]) + a_{b_{24}} (S_{b_{3_z}}^{(4)^2} + S_{b_{3_x}}^{(4)^2} + S_{b_{3_y}}^{(4)^2}) \left(S_{b_{3_z}}^{(4)^2} - \frac{S_{b_{3_x}}^{(4)^2} + S_{b_{3_y}}^{(4)^2}}{2} \right) \end{aligned} \quad (33)$$

$$\begin{aligned}
 S_{b_{2_b}} = & S_{b_{2_b}}^{(1)} - a_{b_{14}} 2 S_{b_{2_a}}^{(2)} S_{b_{2_b}}^{(2)} + a_{b_{15}} \frac{\sqrt{3}}{2} (S_{b_{3_x}}^{(2)^2} - S_{b_{3_y}}^{(2)^2}) + a_{b_{16}} S_{b_{2_b}}^{(3)} (S_{b_{2_a}}^{(3)^2} + S_{b_{2_b}}^{(3)^2}) + a_{b_{17}} S_{b_{2_b}}^{(3)} (S_{b_{3_z}}^{(3)^2} + S_{b_{3_x}}^{(3)^2} + S_{b_{3_y}}^{(3)^2}) \\
 & - a_{b_{18}} 2 S_{b_{2_a}}^{(4)} S_{b_{2_b}}^{(4)} (S_{b_{2_a}}^{(4)^2} + S_{b_{2_b}}^{(4)^2}) + a_{b_{19}} 4 S_{b_{2_a}}^{(4)} S_{b_{2_b}}^{(4)} (S_{b_{2_a}}^{(4)^2} - S_{b_{2_b}}^{(4)^2}) - a_{b_{20}} 2 S_{b_{2_a}}^{(4)} S_{b_{2_b}}^{(4)} (S_{b_{3_z}}^{(4)^2} + S_{b_{3_x}}^{(4)^2} + S_{b_{3_y}}^{(4)^2}) \\
 & + a_{b_{21}} (S_{b_{2_a}}^{(4)^2} + S_{b_{2_b}}^{(4)^2}) \frac{\sqrt{3}}{2} (S_{b_{3_x}}^{(4)^2} - S_{b_{3_y}}^{(4)^2}) + a_{b_{22}} S_{b_{2_b}}^{(4)} S_{b_{3_z}}^{(4)} S_{b_{3_x}}^{(4)} S_{b_{3_y}}^{(4)} \\
 & - a_{b_{23}} \frac{\sqrt{3}}{2} S_{b_{3_z}}^{(4)^2} (S_{b_{3_x}}^{(4)^2} - S_{b_{3_y}}^{(4)^2}) + a_{b_{24}} (S_{b_{3_z}}^{(4)^2} + S_{b_{3_x}}^{(4)^2} + S_{b_{3_y}}^{(4)^2}) \frac{\sqrt{3}}{2} (S_{b_{3_x}}^{(4)^2} - S_{b_{3_y}}^{(4)^2})
 \end{aligned} \tag{34}$$

$$\begin{aligned}
 S_{b_{3_x}} = & S_{b_{3_x}}^{(1)} + a_{b_{25}} S_{b_{3_z}}^{(2)} S_{b_{3_y}}^{(2)} - a_{b_{26}} S_{b_{3_x}}^{(2) \frac{1}{2}} (S_{b_{2_a}}^{(2)} - \sqrt{3} S_{b_{2_b}}^{(2)}) + a_{b_{27}} S_{b_{3_x}}^{(3)^3} + a_{b_{28}} S_{b_{3_x}}^{(3)} (S_{b_{3_z}}^{(3)^2} + S_{b_{3_y}}^{(3)^2}) + a_{b_{29}} S_{b_{3_x}}^{(3)} (S_{b_{2_a}}^{(3)^2} + S_{b_{2_b}}^{(3)^2}) \\
 & - a_{b_{30}} S_{b_{3_x}}^{(3)} \left(\frac{S_{b_{2_a}}^{(3)^2} - S_{b_{2_b}}^{(3)^2}}{2} + \sqrt{3} S_{b_{2_a}}^{(3)} S_{b_{2_b}}^{(3)} \right) - a_{b_{31}} S_{b_{3_y}}^{(3)} S_{b_{3_z}}^{(3)} \frac{1}{2} (S_{b_{2_a}}^{(3)} - \sqrt{3} S_{b_{2_b}}^{(3)}) - a_{b_{32}} S_{b_{3_x}}^{(4)} (S_{b_{2_a}}^{(4)^2} + S_{b_{2_b}}^{(4)^2}) \frac{1}{2} (S_{b_{2_a}}^{(4)} - \sqrt{3} S_{b_{2_b}}^{(4)}) \\
 & + a_{b_{33}} S_{b_{3_x}}^{(4)} (S_{b_{2_a}}^{(4)^3} - 3 S_{b_{2_a}}^{(4)} S_{b_{2_b}}^{(4)^2}) - a_{b_{34}} S_{b_{3_y}}^{(4)} S_{b_{3_z}}^{(4) \frac{1}{2}} (S_{b_{2_a}}^{(4)^2} - S_{b_{2_b}}^{(4)^2} + 2\sqrt{3} S_{b_{2_a}}^{(4)} S_{b_{2_b}}^{(4)}) + a_{b_{35}} S_{b_{3_y}}^{(4)} S_{b_{3_z}}^{(4)} (S_{b_{2_a}}^{(4)^2} + S_{b_{2_b}}^{(4)^2}) \\
 & - a_{b_{36}} S_{b_{3_x}}^{(4) \frac{1}{2}} (S_{b_{2_a}}^{(4)} - \sqrt{3} S_{b_{2_b}}^{(4)}) (S_{b_{3_z}}^{(4)^2} + S_{b_{3_x}}^{(4)^2} + S_{b_{3_y}}^{(4)^2}) - a_{b_{37}} S_{b_{3_x}}^{(4) \frac{3}{2}} (S_{b_{2_a}}^{(4)} - \sqrt{3} S_{b_{2_b}}^{(4)}) \\
 & + a_{b_{38}} S_{b_{3_x}}^{(4)} (S_{b_{3_z}}^{(4)^2} - S_{b_{3_y}}^{(4)^2}) \frac{1}{2} (S_{b_{2_b}}^{(4)} + \sqrt{3} S_{b_{2_a}}^{(4)}) + a_{b_{39}} S_{b_{3_z}}^{(4)} S_{b_{3_y}}^{(4)} (S_{b_{3_z}}^{(4)^2} + S_{b_{3_x}}^{(4)^2} + S_{b_{3_y}}^{(4)^2}) + a_{b_{40}} S_{b_{3_x}}^{(4)} S_{b_{3_z}}^{(4)} S_{b_{3_x}}^{(4)} S_{b_{3_y}}^{(4)},
 \end{aligned} \tag{35}$$

$$\begin{aligned}
 S_{b_{3_y}} = & S_{b_{3_y}}^{(1)} + a_{b_{25}} S_{b_{3_z}}^{(2)} S_{b_{3_x}}^{(2)} - a_{b_{26}} S_{b_{3_y}}^{(2) \frac{1}{2}} (S_{b_{2_a}}^{(2)} + \sqrt{3} S_{b_{2_b}}^{(2)}) + a_{b_{27}} S_{b_{3_y}}^{(3)^3} + a_{b_{28}} S_{b_{3_y}}^{(3)} (S_{b_{3_x}}^{(3)^2} + S_{b_{3_z}}^{(3)^2}) + a_{b_{29}} S_{b_{3_y}}^{(3)} (S_{b_{2_a}}^{(3)^2} + S_{b_{2_b}}^{(3)^2}) \\
 & - a_{b_{30}} S_{b_{3_y}}^{(3)} \left(\frac{S_{b_{2_a}}^{(3)^2} - S_{b_{2_b}}^{(3)^2}}{2} - \sqrt{3} S_{b_{2_a}}^{(3)} S_{b_{2_b}}^{(3)} \right) - a_{b_{31}} S_{b_{3_x}}^{(3)} S_{b_{3_z}}^{(3)} \frac{1}{2} (S_{b_{2_a}}^{(3)} + \sqrt{3} S_{b_{2_b}}^{(3)}) - a_{b_{32}} S_{b_{3_y}}^{(4)} (S_{b_{2_a}}^{(4)^2} + S_{b_{2_b}}^{(4)^2}) \frac{1}{2} (S_{b_{2_a}}^{(4)} + \sqrt{3} S_{b_{2_b}}^{(4)}) \\
 & + a_{b_{33}} S_{b_{3_y}}^{(4)} (S_{b_{2_a}}^{(4)^3} - 3 S_{b_{2_a}}^{(4)} S_{b_{2_b}}^{(4)^2}) - a_{b_{34}} S_{b_{3_x}}^{(4)} S_{b_{3_z}}^{(4) \frac{1}{2}} (S_{b_{2_a}}^{(4)^2} - S_{b_{2_b}}^{(4)^2} - 2\sqrt{3} S_{b_{2_a}}^{(4)} S_{b_{2_b}}^{(4)}) + a_{b_{35}} S_{b_{3_x}}^{(4)} S_{b_{3_z}}^{(4)} (S_{b_{2_a}}^{(4)^2} + S_{b_{2_b}}^{(4)^2}) \\
 & - a_{b_{36}} S_{b_{3_y}}^{(4) \frac{1}{2}} (S_{b_{2_a}}^{(4)} + \sqrt{3} S_{b_{2_b}}^{(4)}) (S_{b_{3_z}}^{(4)^2} + S_{b_{3_x}}^{(4)^2} + S_{b_{3_y}}^{(4)^2}) - a_{b_{37}} S_{b_{3_y}}^{(4) \frac{3}{2}} (S_{b_{2_a}}^{(4)} + \sqrt{3} S_{b_{2_b}}^{(4)}) + a_{b_{38}} S_{b_{3_y}}^{(4)} (S_{b_{3_x}}^{(4)^2} - S_{b_{3_z}}^{(4)^2}) \frac{1}{2} (S_{b_{2_b}}^{(4)} - \sqrt{3} S_{b_{2_a}}^{(4)}) \\
 & + a_{b_{39}} S_{b_{3_x}}^{(4)} S_{b_{3_z}}^{(4)} (S_{b_{3_z}}^{(4)^2} + S_{b_{3_x}}^{(4)^2} + S_{b_{3_y}}^{(4)^2}) + a_{b_{40}} S_{b_{3_y}}^{(4)} S_{b_{3_z}}^{(4)} S_{b_{3_x}}^{(4)} S_{b_{3_y}}^{(4)},
 \end{aligned} \tag{36}$$

$$\begin{aligned}
 S_{b_{3_z}} = & S_{b_{3_z}}^{(1)} + a_{b_{25}} S_{b_{3_x}}^{(2)} S_{b_{3_y}}^{(2)} + a_{b_{26}} S_{b_{3_z}}^{(2)} S_{b_{2_a}}^{(2)} + a_{b_{27}} S_{b_{3_z}}^{(3)^3} + a_{b_{28}} S_{b_{3_z}}^{(3)} (S_{b_{3_x}}^{(3)^2} + S_{b_{3_y}}^{(3)^2}) + a_{b_{29}} S_{b_{3_z}}^{(3)} (S_{b_{2_a}}^{(3)^2} + S_{b_{2_b}}^{(3)^2}) \\
 & + a_{b_{30}} S_{b_{3_z}}^{(3)} (S_{b_{2_a}}^{(3)^2} - S_{b_{2_b}}^{(3)^2}) + a_{b_{31}} S_{b_{3_x}}^{(3)} S_{b_{3_y}}^{(3)} S_{b_{2_a}}^{(3)} + a_{b_{32}} S_{b_{3_z}}^{(4)} S_{b_{2_a}}^{(4)} (S_{b_{3_x}}^{(4)^2} + S_{b_{3_y}}^{(4)^2}) + a_{b_{33}} S_{b_{3_z}}^{(4)} (S_{b_{2_a}}^{(4)^3} - 3 S_{b_{2_a}}^{(4)} S_{b_{2_b}}^{(4)^2}) \\
 & + a_{b_{34}} S_{b_{3_x}}^{(4)} S_{b_{3_y}}^{(4)} (S_{b_{2_a}}^{(4)^2} - S_{b_{2_b}}^{(4)^2}) + a_{b_{35}} S_{b_{3_x}}^{(4)} S_{b_{3_y}}^{(4)} (S_{b_{2_a}}^{(4)^2} + S_{b_{2_b}}^{(4)^2}) + a_{b_{36}} S_{b_{2_a}}^{(4)} S_{b_{3_z}}^{(4)} (S_{b_{3_x}}^{(4)^2} + S_{b_{3_y}}^{(4)^2} + S_{b_{3_z}}^{(4)^2}) \\
 & + a_{b_{37}} S_{b_{2_a}}^{(4)} S_{b_{3_z}}^{(4)^3} + a_{b_{38}} S_{b_{2_b}}^{(4)} S_{b_{3_x}}^{(4)} (S_{b_{3_z}}^{(4)^2} - S_{b_{3_y}}^{(4)^2}) + a_{b_{39}} S_{b_{3_x}}^{(4)} S_{b_{3_y}}^{(4)} (S_{b_{3_z}}^{(4)^2} + S_{b_{3_x}}^{(4)^2} + S_{b_{3_y}}^{(4)^2}) + a_{b_{40}} S_{b_{3_z}}^{(4)} S_{b_{3_z}}^{(4)} S_{b_{3_x}}^{(4)} S_{b_{3_y}}^{(4)}.
 \end{aligned} \tag{37}$$

These expressions have been obtained by reduction of the direct products $A^l \otimes E^m \otimes F^n$ in T_d symmetry (isomorphic to S_4), following the scheme given in Ref. 81 (the appendix). The transformation properties have been tested for each individual equation with MAPLE.⁸²

For the potential models METPOT 3 and METPOT 4, the damping functions introduced in Eq. (20) will have, in principle, different damping parameters $a_{d_l}^{(k)}$ depending on the power order (k) of products of the coordinate $x_{ij}^{(k)}$. The appearance of different bond length functions (e.g., the damping functions, in this case) as a function of the power order of products of bending coordinate displacements is an additional means of introducing implicit stretching–bending interaction potentials. Here, we are describing the influence of different amplitudes of the bending motion on the stretching part of the potential.

For the potential model METPOT 2, the damping parameters do not depend on the power in which products of $x_{ij}^{(k)}$ occur. Instead, $\tilde{a}_{d_l}^{(k)}$ in Eq. (21) has a different meaning: $\tilde{a}_{d_l}^{(1)}$ is used for the coordinate S_{b_1} in Eq. (32), $\tilde{a}_{d_l}^{(2)}$ for S_{b_2} in Eqs. (33) and

(34), and $\tilde{a}_{d_1}^{(3)}$ for S_{b_3} in Eqs. (35)–(37). This approach does not affect the properties of the potential function in regions closer to the equilibrium structure (for which it actually was used in Ref. 73). However, it has some serious disadvantages for the description of the shape of the stretching potential at larger bending amplitudes, and was therefore avoided in the later models.

For METPOT 1, which was the first model potential developed in the context of this work, only $a_{d_2}^{(1)}$ differ from 0. Moreover, for this model, all a_{b_j} were set to zero. In order to describe higher order contributions of larger bending displacements and stretching–bending interaction terms, we had to consider additional cubic and quartic forms:

$$\begin{aligned} \Delta V_b^{\text{METPOT1}} = & F_{b_1^3} S_{b_1}^3 + F_{b_1 b_2^2} S_{b_1} (S_{b_{2a}}^2 + S_{b_{2b}}^2) + F_{b_1 b_3^2} S_{b_1} (S_{b_{3x}}^2 + S_{b_{3y}}^2 + S_{b_{3z}}^2) + F_{b_1^4} S_{b_1}^4 \\ & + F_{b_1^2 b_2^2} S_{b_1}^2 (S_{b_{2a}}^2 + S_{b_{2b}}^2) + F_{a_1^2 b_3^2} S_{b_1}^2 (S_{b_{3x}}^2 + S_{b_{3y}}^2 + S_{b_{3z}}^2) + F_{b_1 b_2^3} S_{b_1} (S_{b_{2a}}^3 - 3S_{b_{2a}} S_{b_{2b}}^2) \\ & + F_{b_1 b_2 b_3^2} S_{b_1} \left\{ S_{b_{2a}} \left(S_{b_{3z}}^2 - \frac{1}{2} (S_{b_{3x}}^2 + S_{b_{3y}}^2) \right) + \frac{\sqrt{3}}{2} S_{b_{2b}} (S_{b_{3x}}^2 - S_{b_{3y}}^2) \right\} \\ & + F_{b_2^4} (S_{b_{2a}}^2 + S_{b_{2b}}^2)^2 + F_{b_2^2 b_3^2} (S_{b_{2a}}^2 + S_{b_{2b}}^2) (S_{b_{3x}}^2 + S_{b_{3y}}^2 + S_{b_{3z}}^2) + F_{b_2^2 b_3^2} \Pi ((S_{b_{2a}}^2 - S_{b_{2b}}^2) (S_{b_{3z}}^2 - \frac{1}{2} (S_{b_{3x}}^2 + S_{b_{3y}}^2))) \\ & - \sqrt{3} S_{b_{2a}} S_{b_{2b}} (S_{b_{3x}}^2 - S_{b_{3y}}^2) + F_{b_3^4} (S_{b_{3x}}^4 + S_{b_{3y}}^4 + S_{b_{3z}}^4) + F_{b_3^4} \Pi (S_{b_{3x}}^2 S_{b_{3y}}^2 + S_{b_{3x}}^2 S_{b_{3z}}^2 + S_{b_{3y}}^2 S_{b_{3z}}^2) + F_{s_1 b_1^2} S_{s_1} S_{b_1}^2 \\ & + F_{s_1 b_2^2} S_{s_1} (S_{b_{2a}}^2 + S_{b_{2b}}^2) + F_{s_1 b_3^2} S_{s_1} (S_{b_{3x}}^2 + S_{b_{3y}}^2 + S_{b_{3z}}^2) + F_{s_1^2 b_1^2} S_{s_1}^2 S_{b_1}^2 + F_{s_1^2 b_2^2} S_{s_1}^2 (S_{b_{2a}}^2 + S_{b_{2b}}^2) \\ & + F_{s_1^2 b_3^2} S_{s_1}^2 (S_{b_{3x}}^2 + S_{b_{3y}}^2 + S_{b_{3z}}^2). \end{aligned} \quad (38)$$

The resulting parameter values are listed in the table of the PAPS supplement 1 (Ref. 96).

In molecules with highly symmetric equilibrium structures like methane (T_d symmetry), infinitesimal displacements of the totally symmetric coordinate $S_{b_1}^{(k)}$ vanish identically at equilibrium: $dS_{b_1}^{(k)} = \sum_{i>j} dx_{ij}^{(k)}|_{r_1=r_e, \dots, r_4=r_e} = \sum_{i>j} d \cos(\alpha_{ij}) = 0$ (the reason being the redundancy condition for the six valence angles). Displacements from equilibrium are thus only of quadratic order in S_{b_1} , which makes potential contributions originating from $S_{b_1}^2$ to be at least of quartic order. However, we may conclude from this, that in methane an additional contribution to the quadratic force field may exist, which is proportional to a linear term in S_{b_1} . We define

$$S_{b_0} = \sum_{i<j} (\cos(\alpha_{ij}) - c_e) y_d^{(0)}(r_i) y_d^{(0)}(r_j), \quad (39)$$

where c_e is the cosine of the equilibrium angle and, like r_e , a slowly varying function of the bond lengths. The index (0) characterizes the use of special damping parameters for this coordinate. It was checked numerically that S_{b_0} is always positive definite, when all bond lengths are at equilibrium.

For METPOT 2, METPOT 3, and METPOT 4, the final form of the bending potential is

$$\begin{aligned} V_{b(YXY)} = & F_{b_0} S_{b_0} + F_{b_1} S_{b_1}^2 + F_{b_2} (S_{b_{2a}}^2 + S_{b_{2b}}^2) \\ & + F_{b_3} (S_{b_{3x}}^2 + S_{b_{3y}}^2 + S_{b_{3z}}^2). \end{aligned} \quad (40)$$

The ‘‘coordinates’’ (S_{b_0} to S_{b_3}) have been defined in Eqs. (39) and (32)–(37). For METPOT 1, one has to add the expression in Eq. (38) to it.

In the limit $r_i \rightarrow \infty$ and planar equilibrium structure for the CH_3 frame (the case for the methyl radical), the potential term proportional to F_{b_0} gives the quadratic force field of the A_2'' out-of-plane mode, e.g., for $r_1 \rightarrow \infty$:

$$\begin{aligned} \Delta \cos(\alpha_{23}) + \Delta \cos(\alpha_{24}) + \Delta \cos(\alpha_{34}) \\ = \frac{3}{2} (2 \cos(\alpha) + 1) = \frac{9}{2} \frac{z^2}{r_e^2}, \end{aligned} \quad (41)$$

where $\alpha_{23} = \alpha_{24} = \alpha_{34} \equiv \alpha$, for this mode, and z is the vertical distance of the H_3 plane from the C atom (as used by Riveros⁸³ and Yamada *et al.*⁶⁷).

D. The H–H pair potential

The direct (two-body) interaction potential between two peripheral H atoms has been studied in Ref. 36. For the purpose of the present work, it is sufficient to use the normal Morse potential as a function of the interatomic distance r_{ij} . In the models METPOT 2, METPOT 3, and METPOT 4 we define:

$$\begin{aligned} V_{ij} = & D_{ij} (\dots r_k \dots) (1 - \exp(-a_{ij} (\dots r_k \dots)))^2 \\ & \times [r_{ij} - r_{ij}^{\text{eq}} (\dots r_k \dots)]. \end{aligned} \quad (42)$$

Here, D_{ij} , a_{ij} , and r_{ij}^{eq} are the following functions of the CH bond lengths:

$$r_{ij}^{\text{eq}} = r_{\text{HH}} [1 - S_{p_{r_{\text{HH}}}}(r_i) S_{p_{r_{\text{HH}}}}(r_j)] + r_{\text{HH}}^{\infty} S_{p_{r_{\text{HH}}}}(r_i) S_{p_{r_{\text{HH}}}}(r_j), \quad (43)$$

$$a_{ij} = a_{\text{HH}} [1 - S_{p_{a_{\text{HH}}}}(r_i) S_{p_{a_{\text{HH}}}}(r_j)] + a_{\text{HH}}^{\infty} S_{p_{a_{\text{HH}}}}(r_i) S_{p_{a_{\text{HH}}}}(r_j), \quad (44)$$

$$D_{ij} = D_{\text{HH}} [1 - S_{p_{D_{\text{HH}}}}(r_i)] [1 - S_{p_{D_{\text{HH}}}}(r_j)] + D_{\text{HH}}^{\infty} S_{p_{D_{\text{HH}}}}(r_i) S_{p_{D_{\text{HH}}}}(r_j). \quad (45)$$

The equilibrium H–H length is defined by $r_{\text{HH}} = \sqrt{r_i^{\text{eq}2} + r_j^{\text{eq}2} - 2r_i^{\text{eq}}r_j^{\text{eq}}c_{ij}^{\text{eq}}}$, where r_i^{eq} and c_{ij}^{eq} have been defined previously in Eqs. (17) and (25) [for METPOT 2, r_{HH} was calculated with r_e and c_e and D_{ij} changes with r_i and r_j in the same way as a_{ij} in Eq. (44)]. a_{HH} and D_{HH} are slowly varying parameters, r_{HH}^{∞} , a_{HH}^{∞} , and D_{HH}^{∞} are the parameters of a Morse potential for the isolated hydrogen molecule. The functions $S_{p_{r_{\text{HH}}}}$, $S_{p_{a_{\text{HH}}}}$ and $S_{p_{D_{\text{HH}}}}$ are switching functions, chosen here to be of the type

$$S_{p_x}(r) = \exp\left(-\left(\frac{r_x}{r}\right)^{n_x}\right) \quad (46)$$

and to be discussed in sec. III E below (“ x ” = “ r_{HH} ,” “ a_{HH} ,” and “ D_{HH} ”).

For the potential model METPOT 1, we used a slightly different definition, in which

$$V_{ij} = V_{ij}^0 + (V_{ij}^{\infty} - V_{ij}^0) S_{p_{D_{\text{HH}}}}(r_i) S_{p_{D_{\text{HH}}}}(r_j), \quad (47)$$

where

$$V_{ij}^0 = D_{\text{HH}} (1 - \exp(-a_{\text{HH}} [r_{ij} - r_{ij}^{\text{eq}} (\cdots r_k \cdots)]))^2 \quad (48)$$

and

$$V_{ij}^{\infty} = D_{\text{HH}}^{\infty} (1 - \exp(-a_{ij} (\cdots r_k \cdots) [r_{ij} - r_{\text{HH}}^{\infty}]))^2 \quad (49)$$

with

$$a_{ij} = a_{\text{HH}}^{\infty} + \delta a_{\text{HH}} \exp(-p_{a_{\text{HH}}} [(r_i - r_{a_{\text{HH}}}) + (r_j - r_{a_{\text{HH}}})]). \quad (50)$$

In the limit of simultaneous bond ruptures $r_i \rightarrow \infty$ and $r_j \rightarrow \infty$, the H₂-binding energy needs to be subtracted from the total energy. We consider increasingly negative energy terms V_{ij}^{rep} with increasing CH-bond lengths (these terms are thus of a repulsive character). For METPOT 1,

$$V_{ij}^{\text{rep}} = -D_{\text{HH}}^{\infty} \rho_{\text{HH}}^{\infty} S_{p_{D_{\text{HH}}}}(r_i) S_{p_{D_{\text{HH}}}}(r_j), \quad (51)$$

for METPOT 2 [see Eq. (45)],

$$V_{ij}^{\text{rep}} = -D_{ij}, \quad (52)$$

for METPOT 3 and 4:

$$V_{ij}^{\text{rep}} = -D_{\text{HH}}^{\infty} S_{p_{D_{\text{HH}}}}(r_i) S_{p_{D_{\text{HH}}}}(r_j) \times \prod_{k \neq (i,j)} S_{p_{D_{\text{HH}}}}(r_{ik}) S_{p_{D_{\text{HH}}}}(r_{jk}). \quad (53)$$

One result of our investigations is that, typically, $D_{\text{HH}}^{\infty} \gg D_{\text{HH}}$. Also, the maximal decrease rate of V_{ij}^{rep} is not larger than the increase rate of the potential D_{ij} in Eq. (45).

The subsequent subtraction of the H₂ binding energies in the asymptotic limit of three and more bond ruptures could lead to deep unphysical energy minima on the global potential surface for CH₄, if no further positive interaction energy between the dissociated H_m aggregates is considered. In order to avoid this, we considered, in the models METPOT 3 and METPOT 4, the factor $\prod_{k \neq (i,j)} S_{p_{D_{\text{HH}}}}(r_{ik}) S_{p_{D_{\text{HH}}}}(r_{jk})$ in

Eq. (53), which “turns off” the repulsive potential for the pair (ij) of H atoms, whenever a third H atom comes too close to it. Of course, for the correct description of the (repulsive) H_n potential for $n \geq 3$, the model should describe explicitly many-body interaction terms between the individual H atoms (this is also valid for molecules of the general type XY_n, when Y_m clusters need to be described in addition to Y₂). In the present work, such interactions have not been considered.

For the potential models METPOT 1 and METPOT 2, the subtraction of H₂-binding energies, when more than two H atoms dissociate, was not avoided. Instead, a positive potential V_{H_m} was added to V_{ij}^{rep} , which balances this effect. For METPOT 1:

$$V_{H_m} = 2D_{\text{HH}}^{\infty} \sum_j \prod_{i \neq j} S_{p_{D_{\text{HH}}}}(r_i), \quad (54)$$

for METPOT 2:

$$V_{H_m} = 2D_{\text{HH}}^{\infty} \sum_j \prod_{i \neq j} S_{p_{D_{\text{HH}}}}(r_i) \times \sum_{k \neq j, l \neq j, l > k} \exp\left(-\frac{1}{2} a_{kl} (r_{kl} - r_{kl}^{\text{eq}})\right). \quad (55)$$

The total pair potential is the total symmetric sum

$$V_{s(Y Y)} = \sum_{i=1}^n \sum_{j>i}^n (V_{ij} + V_{ij}^{\text{rep}}) + V_{H_m} \quad (56)$$

($V_{H_m} = 0$ for METPOT 3 and 4).

E. Switching functions

One requirement made to global model potentials is that all dissociation channels need to be described in a correct way within the same analytical representation (for single or multiple valued potential surfaces). This implies conditions both on the symmetry aspects of the representations and parameter values for the models.

The expressions for the potential function derived in the present work are the most general quadratic forms which are totally symmetric with respect to permutations of coordinates of Y atoms occurring in S₄. For sequential atomizations,

$$XY_n \rightarrow XY_{n-1} + Y, \quad (57)$$

$$XY_{n-1} \rightarrow XY_{n-2} + Y, \quad (58)$$

⋮

the following relationship holds:

$$\begin{array}{ccccccc} XY_4 & \rightarrow & XY_3 + Y & \rightarrow & XY_2 + 2Y & \rightarrow & XY + 3Y, \\ S_4 & \supset & S_3 & \supset & S_2 & \supset & S_1 \\ \wr & & \wr & & \wr & & \wr \\ & & C_{3v} & & C_{2v} & & \\ T_d & \supset & & \supset & & \supset & \text{“}C_1\text{”} \\ & & D_{3h} \setminus \{i\} & & D_{\infty h} \setminus \{i, \text{Rot}\} & & \end{array} \quad (59)$$

In this diagram, a tilde (\sim) means the isomorphism between the symmetric group S_n and the molecular point group or its corresponding subgroup. S_3 is isomorphous to C_{3v} , for instance, and isomorphous to the subgroup $D_{3h}\setminus\{i\}$ of D_{3h} that does not contain the inversion operation. This relationship is specifically important in the context of sequential atomizations of XY_n compounds with equivalent interatomic interactions such as CH_4 , CH_3 , and NH_3 . For instance for these compounds, the equilibrium molecular point groups are T_d , D_{3h} , and C_{3v} . The quadratic forms of the potential after the j th atomization step can be considered to be the most general ones having the local molecular point group symmetry of the product molecule XY_{n-j} except for the inversion operation. However, the latter can be successfully described by the linear totally symmetric sum of angle coordinates, as discussed above.

Thus, the analytical representation derived for S_4 automatically generates formally correct representations for all subgroups and may be used to describe the potential surfaces of CH_3 , CH_2 , and CH , as well as, e.g., for NH_3 , NH_2 , NH , CO_2 , and H_2O . For compounds with nonequivalent interatomic interactions such as CH_4^+ or O_3 , the present representation may also be used, if some extensions of the formalism are considered, which include the use of interaction specific interatomic coordinates, but will not be further discussed here.

For quantitatively correct descriptions, the parameter values need to change after subsequent atomizations. Here, we use switching functions of the bond lengths, since these coordinates best describe the status of the system at different atomization levels. In particular, we use functions of the type [see also Eq. (46)].

$$S_{p_{sw}}(r) = \exp\left(-\left(\frac{r_{sw}}{r}\right)^{n_{sw}}\right), \quad (60)$$

$$S_{q_{sw}}(r) = 1 - S_{p_{sw}}(r). \quad (61)$$

In these equations, sw characterizes a certain parameter or parameter group, to which the switching function $S_{p_{sw}}$ is applied, r_{sw} and n_{sw} are corresponding parameters for the switching function. In METPOT 1 and METPOT 2, we considered the three parameter groups: r_e (sw = r_e), all stretching parameters (sw = str) and all bending and pair potential parameters (sw = bend) (see Tables PAPS supplement 1 and PAPS supplement 2). However, as demonstrated by the present model METPOT 3 and METPOT 4, a single switching function (with parameters r_{sw} and n_{sw} in Table PAPS supplement 3) is sufficiently flexible for the description of the global surface. This function is shown in Fig. 2, with typical values for the switching parameters.

The functions introduced here have the advantage of being really logical (01-) switching functions on the whole definition range of their arguments. For switching parameter values $n_{sw} \geq 6$ and $r_{sw} \geq \sqrt{2}r_e$, which are found to be realistic ranges for the investigated compounds, one obtains $1 > S_{q_{sw}}(r) > 0.999$ for $r \leq r_e$. For other types of switching

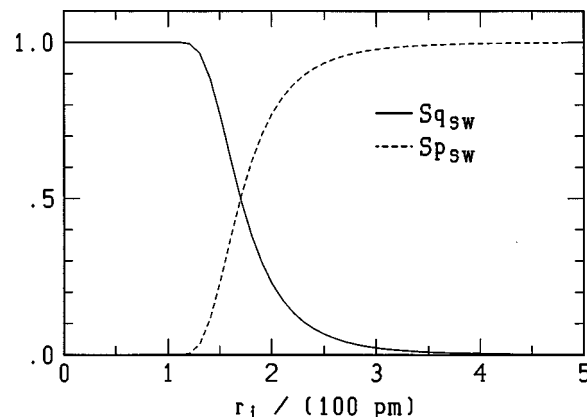


FIG. 2. Switching functions $S_{p_{sw}}$ and $S_{q_{sw}}$ with $n_{sw}=8$ and $r_{sw}=2.0 \text{ \AA}$.

functions used in the literature (e.g., with the arctan or tanh function used in Eqs. (26) and (27), see also Refs. 2 and 78), one usually has $S_{q_{sw}}(r) > 1$ (even $S_{q_{sw}}(r) \gg 1$ is possible), for $r < r_e$, in which case some parameter values may become negative, e.g., F_s or F_b . In contrast, logical switching functions are helpful in setting up multidimensional switching surfaces, which were finally used throughout this work to construct global potential surfaces. The diagram shown in Fig. 3 illustrates this procedure for methane [the parameter ‘‘P’’ may be switched to four different values, in practice, $P(5)$ being irrelevant in most cases].

F. Harmonic force field and further analytical constraints

The relationship between the representation of the global potential surface and the harmonic force field of methane, the methyl and methylene radicals is important for the determination of empirically refined parameter sets. As will be discussed below, the parameter adjustment to the *ab initio* data can be performed under simultaneous consideration of additional constraints, such as the experimental harmonic force field. It is of great help to determine the relevant expressions analytically, which was performed here with MAPLE.⁸²

The potential surface can be expanded as a polynomial in displacement coordinates from equilibrium, the lowest nonvanishing terms being of quadratic order:

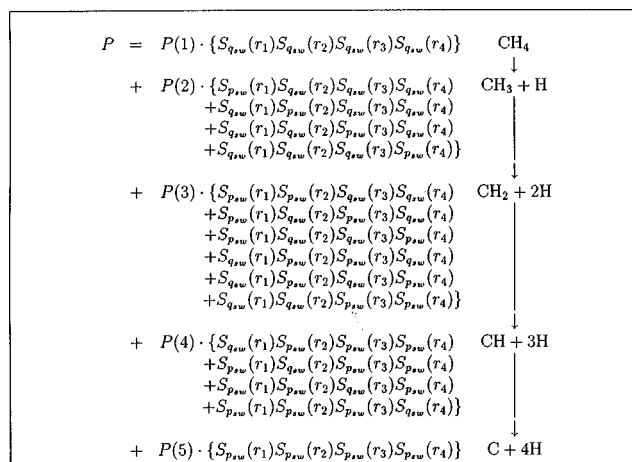


FIG. 3. Diagram for switching parameters in CH_n potential surfaces as a function of bond lengths in CH_4 .

$$V = \frac{1}{2} \sum_{i,j} F_{ij} s_i s_j + \dots \quad (62)$$

The s_i are symmetrized displacement coordinates. For methane, they have been defined, e.g., in Refs. 10, 12, and 84.

The harmonic force field F_{ij} of these compounds is given by the following expressions of the model parameters from the present work (METPOT 3 and 4). For methane,

$$F_{11} = F_s(1)(1 - 3g_r(1))^2 + 2F_{b_1}(1)a_c(1)^2 + 8D_{\text{HH}}(1)a_{\text{HH}}(1)^2(1 - 3g_r(1) - \frac{1}{8}r_e(1)a_c(1))^2, \quad (63)$$

$$F_{22} = \frac{64}{9}F_{b_2}(1) + \frac{2}{3}D_{\text{HH}}(1)a_{\text{HH}}(1)^2r_e(1)^2, \quad (64)$$

$$F_{33} = F_s(1)(1 + g_r(1))^2 + \frac{2}{9}F_{b_3}(1)a_c(1)^2 + \frac{8}{3}D_{\text{HH}}(1)a_{\text{HH}}(1)^2(1 + g_r(1) + \frac{1}{8}r_e(1)a_c(1))^2, \quad (65)$$

$$F_{34} = -\frac{4}{3}F_{b_0}(1)a_{d_1}^{(0)}(1)(1 + g_r(1)) - \frac{8}{9}F_{b_3}(1)a_c(1) - \frac{4}{3}D_{\text{HH}}(1)a_{\text{HH}}(1)^2r_e(1)(1 + g_r(1) + \frac{1}{8}r_e(1)a_c(1)), \quad (66)$$

$$F_{44} = \frac{4}{3}F_{b_0}(1) + \frac{32}{9}F_{b_3}(1) + \frac{2}{3}D_{\text{HH}}(1)a_{\text{HH}}(1)^2r_e(1)^2. \quad (67)$$

For the methyl radical,

$$F_{11} = F_s(2)(1 - 2g_r(2))^2 + 2(3F_{b_1}(2) + F_{b_3}(2))a_c(2)^2[c_e(3) + \frac{1}{2}]^2 + 6D_{\text{HH}}(2)a_{\text{HH}}(2)^2(1 - 2g_r(2) + [2c_e(3) + 1]\frac{1}{6}r_e(2)a_c(2))^2, \quad (68)$$

$$F_{22} = 9F_{b_0}(2), \quad (69)$$

$$F_{33} = F_s(2)(1 + g_r(2))^2 + 2(2F_{b_2}(2) + F_{b_3}(2))a_c(2)^2[c_e(3) + \frac{1}{2}]^2 + \frac{3}{2}D_{\text{HH}}(2)a_{\text{HH}}(2)^2(1 + g_r(2) - [2c_e(3) + 1]\frac{1}{3}r_e(2)a_c(2))^2, \quad (70)$$

$$F_{34} = -\frac{\sqrt{3}}{2}F_{b_0}(2)a_{d_1}^{(0)}(2)(1 + g_r(2)) + \sqrt{3}(2F_{b_2}(2) + F_{b_3}(2))a_c(2)[c_e(3) + \frac{1}{2}] - \frac{\sqrt{3}}{2}D_{\text{HH}}(2)a_{\text{HH}}(2)^2r_e(2)(1 + g_r(2) - [2c_e(3) + 1]\frac{1}{3}r_e(2)a_c(2)), \quad (71)$$

$$F_{44} = \frac{1}{2}F_{b_0}(2) + \frac{3}{2}(2F_{b_2}(2) + F_{b_3}(2)) + \frac{1}{2}D_{\text{HH}}(2)a_{\text{HH}}(2)^2r_e(2)^2, \quad (72)$$

$$F_{24} = 54D_{\text{HH}}(2)r_e(2)^2a_{\text{HH}}(2)^2 + 486F_{b_1}(2) + 162F_{b_3}(2). \quad (73)$$

For methylene,

$$F_{11} = F_s(3)(1 - g_r(3))^2 + 2D_{\text{HH}}(3)a_{\text{HH}}(3)^2 \times [1 - c_e(3)](1 - g_r(3))^2, \quad (74)$$

$$F_{12} = \sqrt{2}D_{\text{HH}}(3)a_{\text{HH}}(3)^2r_e(3)(1 - g_r(3))\sqrt{1 - c_e(3)^2}, \quad (75)$$

$$F_{22} = 2(F_{b_1}(3) + \frac{4}{3}F_{b_2}(3) + F_{b_3}(3))[1 - c_e(3)^2] + D_{\text{HH}}(3)a_{\text{HH}}(3)^2r_e(3)^2[1 + c_e(3)], \quad (76)$$

$$F_{33} = F_s(3)(1 + g_r(3))^2. \quad (77)$$

In these equations, the values $c_e(1) = -1/3$, $c_e(2) = -1/2$ have been considered implicitly, and $g_r(n)$ is defined as $a_r(n)(r_e(n+1) - r_e(n))$.

During the adjustment of the bending ‘‘anharmonicity’’ parameters $a_{b_j}(1)$ in methane, we found it convenient to impose the condition

$$\frac{\partial V_{b(YXY)}}{\partial \varphi} = 0, \quad (78)$$

where φ is the azimuthal angle described in Fig. 1. The physical motivation is that the bending potential $V(\vartheta, \varphi)$ has nearly $C_{\infty v}$ symmetry (see Fig. 1 for the definition of the angular coordinates): $V(\vartheta, \varphi) \approx V(\vartheta)$ (for $\vartheta \leq 60^\circ$). The cosine of the valence angles can be written as closed analytical expressions of the angles ϑ and φ from Fig. 1 and $V_{b(YXY)}$ can be evaluated as an analytical function of these angles (e.g., with MAPLE). In order that Eq. (78) be valid, we found that the following equations must necessarily hold:

$$0 = 12\sqrt{3}a_{b_5}(1) + 6\sqrt{3}a_{b_6}(1) + a_{b_7}(1), \quad (79)$$

$$0 = 6a_{b_{11}}(1) + 2a_{b_{12}}(1) - a_{b_{13}}(1), \quad (80)$$

$$0 = 4a_{b_{14}}(1) + a_{b_{15}}(1), \quad (81)$$

$$0 = 4a_{b_{18}}(1) + a_{b_{21}}(1), \quad (82)$$

$$0 = a_{b_{19}}(1), \quad (83)$$

$$0 = 4a_{b_{20}}(1) + a_{b_{24}}(1), \quad (84)$$

$$0 = a_{b_{23}}(1), \quad (85)$$

$$0 = a_{b_{24}}(1), \quad (86)$$

$$0 = a_{b_{25}}(1) + \sqrt{3}a_{b_{26}}(1), \quad (87)$$

$$0 = a_{b_{27}}(1) - a_{b_{28}}(1) + 3a_{b_{30}}(1), \quad (88)$$

$$0 = \sqrt{3}a_{b_{30}}(1) + a_{b_{31}}(1), \quad (89)$$

$$0 = \sqrt{3}a_{b_{32}}(1) + a_{b_{35}}(1), \quad (90)$$

$$0 = a_{b_{33}}(1) + \frac{\sqrt{3}}{36}a_{b_{40}}(1), \quad (91)$$

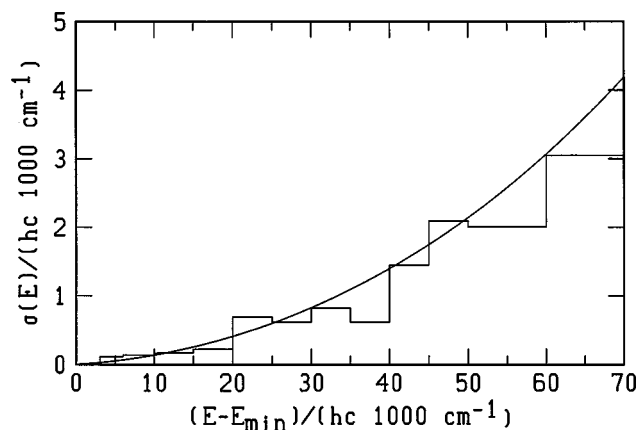


FIG. 4. Estimation of uncertainties of the MRD-CI *ab initio* energies from Eq. (1) and histogram of deviation frequencies in given energy ranges from the adjustment of potential METPOT 3 to the *ab initio* data.

$$0 = a_{b_{34}}(1), \quad (92)$$

$$0 = \sqrt{3}a_{b_{36}}(1) + a_{b_{39}}(1), \quad (93)$$

$$0 = a_{b_{37}}(1), \quad (94)$$

$$0 = a_{b_{38}}(1). \quad (95)$$

We have also determined a constraint on the parameters $a_{b_j}(3)$ by fixing the barrier height to linearity for methylene [it is sufficient to choose $F_{b_1}(3)$ as the only nonvanishing force constant in $V_{b(YXY)}$]:

$$\begin{aligned} V_{\text{barrier}}(\text{CH}_2) &\approx F_{b_1}(3)([1 + c_e(3)] - a_{b_1}(3)[1 + c_e(3)]^2 \\ &\quad + a_{b_4}(3)[1 + c_e(3)]^3)^2 + D_{\text{HH}}(3) \\ &\quad \times (\exp(-a_{\text{HH}}(3)r_e(3)[2 - \sqrt{2}\sqrt{1 - c_e(3)}]) - 1)^2. \end{aligned} \quad (96)$$

IV. DISCUSSION OF ADJUSTMENT PROCEDURES

The model parameters were determined by adjustment of the model potential in Eq. (4) to the *ab initio* data described in Sec. II with the Marquardt algorithm⁸⁵ in which

$$\chi^2 = \frac{1}{n_{\text{data}}} \sum_{n=1}^{n_{\text{data}}} \frac{(E_n^{\text{ab initio}} - E_n^{\text{model}})^2}{\sigma_n^2} \quad (97)$$

is minimized. The *ab initio* data were weighted, the weights being reciprocal to the ‘‘uncertainties’’ given in Sec. II, Eq. (1), which we show in Fig. 4.

When adjusting the parameters to the *ab initio* data without further constraint, we obtain a potential representation which has too large an equilibrium CH bond length and harmonic frequencies much higher than what is expected from experiment (analogous to previous findings in Refs. 11, 68, and 86). In order to improve the model potential, we have considered additional conditions as ‘‘experimental refinements.’’ First, the ‘‘*ab initio*’’ surface was scaled by multiplying the values of the CH bond lengths used in Sec. II with the factor 0.993 69. This factor is the ratio of the equilibrium

CH bond length of methane derived from experimental data (1.0858 Å^{10,64}) to the equilibrium value obtained in Sec. II.

Second, the harmonic force field is adjusted to be identical to Gray and Robiette’s result.¹⁰ For this purpose, the functional forms given in Eqs. (63) to (67) in Sec. III F have been considered as analytical conditions C_i by introduction of Lagrange multipliers μ_i in a modified version of the optimization algorithm from Ref. 85, in which

$$\chi'^2 = \chi^2 + \sum_i \mu_i C_i \quad (98)$$

is minimized. The coefficients F_{ij} on the left-hand side of Eqs. (63)–(67) are given by the values from Ref. 10. Similarly, the functional forms in Eqs. (68)–(72) were considered for the harmonic force field of the methyl radical with values from Refs. 67 and 87, and Eqs. (74)–(77) for the methylene radical, with values from Ref. 88. For the methyl radical, we also considered the quartic force field coefficient of the A_2'' out-of-plane bending vibration [e.g., in Eq. (73)] from Ref. 67, which agrees well with data from Ref. 77. The results in Ref. 87 are not in agreement with the previous findings of the same authors in Ref. 67. The harmonic force field of the methyl radical seems, indeed, not yet to be well determined.^{89,90} For CH₂, the barrier to linearity, as given in Eq. (96), was also considered, with values from Refs. 91 and 92.

Additional analytical conditions are given by the dissociation energies in Eq. (10). First estimations of D_e have been obtained from experimental data for D_0 in Ref. 63 (in good agreement with data from Refs. 66, 93–95, see also Ref. 25, 26) and the harmonic zero point energies (data for H₂ were taken from Ref. 63). A discussion of the use of harmonic zero point energies and possible corrections from anharmonicity effects will be given in a subsequent paper⁵³ (for methane, corrections turn out to be very small, on the order of 0.5 kJ mol⁻¹ or 0.0008 aJ which is mainly due to cancellations).

Further analytical conditions could be imposed, in principle, by comparison of the anharmonic force field with data from experimental results. For this purpose, functional forms of the parameters, similar to those derived for the harmonic force field in Sec. III F, need to be calculated. These would then involve parameters like the stretching (a_s) and bending (a_b) ‘‘anharmonicities.’’ The latter cannot be easily determined from the present *ab initio* data set, although they will prove to be most important for the description of large amplitude bending motions. In the present work, we make a different assumption, given by Eq. (78) [i.e., Eqs. (79) to (89)]. A resulting azimuthal dependence of the total potential will be due, in the present model, to the H–H pair potential, and is expected to be small at moderate values of ϑ .

An important experimental refinement of the model potential is achieved by indirect consideration of the experimental overtone spectrum of the CH chromophore in CHD₃. This makes the difference between the models METPOT 3 and METPOT 4 and will be discussed in detail in a following paper. In METPOT 4 the experimental overtone spectrum was used to refine the potential surface.

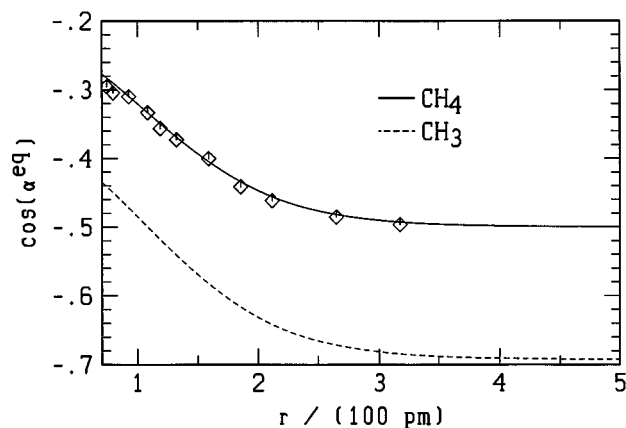


FIG. 5. Optimized HCH-angle during the reaction $\text{CH}_4 \rightarrow \text{CH}_3 + \text{H}$ (continuous line), shown as function c_{ij}^{eq} of the CH bond length [Eq. (25)] with $a_c = 0.912461 \text{ \AA}^{-1}$; \diamond are data from Refs. 55–57; the broken lower curve is the expected angle variation for the reaction $\text{CH}_3 \rightarrow \text{CH}_2 + \text{H}$.

The resulting parameter sets from the present work are collected in Table PAPS supplement 3.⁹⁶ The parameter sets used in our previous work are also given here, for completeness, in the Tables PAPS supplement 1 and PAPS supplement 2.⁹⁶ In these tables, a reference is given for each parameter to the equation where it is defined. As discussed in Sec. III, the analytical representations METPOT 1 and METPOT 2 are slightly different and somewhat more difficult to treat than the present model potential. Therefore, results from these representations will be less addressed in the remainder of this discussion.

Both for METPOT 3 and METPOT 4, 43 parameters have been varied for the description of the potential surface in the definition domain of the CH_4 molecule. The variation of those bending “anharmonicity” parameters a_{b_j} involving fourth-order contributions to S_{b_n} in Eqs. (32)–(37) (higher than sixth power order in V_b) has not led to a significant improvement of the models. In practice, for the present results, these parameters have been set to zero (only 18 of the 40 parameters a_b have been varied: a_{b_1} to a_{b_7} , $a_{b_{14}}$ to $a_{b_{17}}$ and $a_{b_{25}}$ to $a_{b_{31}}$). Fifteen additional constraints, given as analytical equations for the parameters, have been considered during the adjustment. The parameters r_s , r_{sw} , n_{sw} , a_{HH} and $r_{a_{\text{HH}}}$ were varied manually. a_c was determined by an independent adjustment of the function $c_{23}^{\text{eq}}(r_1)$ [Eq. (25)] to a subset of the *ab initio* data (from Refs. 55–57) which describe the optimized α_{23} angle ($=\alpha_{24}=\alpha_{34}$) as a function of r_1 . The quality of this adjustment is shown in Fig. 5. Thus, effectively, 25 parameters have been varied. In the present work, the harmonic force field of CH_3 , CH_2 , and CH is given by experimental values, and many of the anharmonicity parameters were essentially taken from the adjusted CH_4 values (apart from the out-of-plane bending in CH_3 and the bending in CH_2 , which were adjusted to experimental results from the literature). Switching parameters were considered to be identical for all compounds.

Standard deviations for individual parameters as a measure of the statistical uncertainty in their determination cannot, in general, be extracted from the adjustment algorithm,

when additional conditions are considered, because these conditions impose also a large correlation between the parameters involved, in addition to the analytical fitting bias. For METPOT 3, the averaged weighted deviation χ of the adjustment to all data up to 2 aJ is 0.0021 aJ (107 cm^{-1}), the unweighted deviation is 0.028 aJ. The averaged unweighted deviation for roughly 150 data up to 0.4 aJ ($\sim 20\,000 \text{ cm}^{-1}$) is 0.0030 aJ. For 450 data up to 0.8 aJ (roughly the dissociation energy), the averaged weighted deviation is 0.0019 aJ, the averaged unweighted deviation is 0.015 aJ, the largest deviation is 0.08 aJ. In Fig. 4, mean (unweighted) deviations per energy range (deviation frequencies) are shown in a histogram, from which one can see that, e.g., the averaged deviation in the range between $30\,000$ and $35\,000 \text{ cm}^{-1}$ is 820 cm^{-1} (0.016 aJ). Roughly, these values follow the uncertainty function Eq. (1) of the *ab initio* data. For METPOT 4, the averaged weighted deviation to all *ab initio* data up to 2 aJ is 12% higher than for METPOT 3 (roughly 120 cm^{-1}).

In a subsequent paper,⁵³ we shall discuss the quality of the potential surface models for methane by showing some graphical representations of one- and two-dimensional cuts of the global potential hypersurface and comparing the results with corresponding cuts of other model potential functions from the literature. These cuts will also show that the overall functions are indeed very smooth, and that the potential surface METPOT 4 is lower than METPOT 3 in almost all regions. The parameter values given in the PAPS Supplement⁹⁶ have been written with as many digits as necessary to calculate those results. We draw attention also to recent work from our group, where the small parity violating potentials due to the weak nuclear interaction have been calculated for methane.⁹⁷

V. CONCLUSIONS

Effective potential energy hypersurfaces for the nuclear motion in molecular systems, such as those derived from the Born–Oppenheimer approximation for the solution of the molecular Schrödinger equation, constitute an important instrument for the investigation and understanding of the molecular structure and dynamics. Applications are found in many different fields, such as spectroscopy and chemical kinetics. Global potential energy hypersurfaces may be considered as bridges between these fields. They allow, on the one hand, for an insightful evaluation of experimental data, on the other hand they help to understand the connected set of individually calculated *ab initio* potential points.

The representation of potential surfaces through analytical model potentials is of special interest. Analytical representations can be useful, compact summaries of the huge amount of data from *ab initio* theory needed to describe the nuclear motion in polyatomic molecules. They also help to obtain a meaningful interpretation of the potential hypersurface, a physically correct interpolation, occasionally also the extrapolation of *ab initio* data points to asymptotic regions of configuration space. And, most important, analytical representations may be adjusted to experimental results.

For covalently bound polyatomic molecules, the derivation of adequate analytical representations of potential surfaces is a difficult task. Common representations are either

not sufficiently flexible, or not robust. A lack of flexibility usually hinders a better description of experimental data. A lack of robustness has often caused in the past the creation of physical artifacts in regions of the multidimensional surface, which had not been well constrained. Robust and flexible representations may be obtained from compact functional forms of the internal coordinates, which already contain a great part of the specific interaction.

In the present work, we have developed analytical representations of potential hypersurfaces under special consideration of the criteria globality, flexibility, and robustness. The formulas derived in Sec. III are of a rather general type and can be used to describe the potential surface of a general compound XY_n , after some extensions. The possibilities for obtaining more generalized forms under the given symmetry constraints have not been exhausted yet. The representations have been applied to derive model potentials which describe the (globally) lowest electronic state of methane and its dissociation products. Parameter values have been determined, in a first, raw procedure, by fitting the model potential to a large set of *ab initio* energy points. In a second, "fine tuning" step, the model potential was refined empirically, without changing the coarse shape of the potential surface, to yield results that agree much better with experimental observables. For this purpose, several quantities such as the experimental CH bond length, the harmonic force field, the dissociation energies, and the experimentally determined anharmonic model potential surface of the CH chromophore in CHD_3 have been considered as additional constraints during the final fits. Certain additional conditions have been considered directly by introduction of Lagrange multipliers in the least-squares algorithm. Four slightly different model potentials have been determined: METPOT 1 to METPOT 4. The first two have already been referred to in our previous works.^{64,71–73} The methane model potential METPOT 4 can be considered to be a best compromise. We will discuss its application to various experimental quantities in a subsequent paper.⁵³

ACKNOWLEDGMENTS

Help from and discussions with Marius Lewerenz in the early stage of this work are gratefully acknowledged, as well as discussions with T. K. Ha, D. Luckhaus, J. Stohner, M. Suhm, and I. Thanopoulos. Our work is supported financially by the Schweizerischer Nationalfonds and ETH-Zürich (including also C4 project).

¹H. Eyring and M. Polanyi, *Z. Phys. Chem. Abt. B* **12**, 279 (1931).

²J. N. Murrell, S. Carter, S. C. Farantos, P. Huxley, and A. J. C. Varandas, *Potential Energy Functions* (Wiley, New York, 1984).

³G. C. Schatz, *The Analytic Representation of Potential Energy Surfaces for Chemical Reactions*, in *Advances in Molecular Electronic Structure Theory*, Vol. 1, edited by T. H. Dunning, Jr. (JAI, Greenwich, CT, 1990), pp. 85–127.

⁴M. Quack and M. A. Suhm, *J. Chem. Phys.* **95**, 28 (1991).

⁵M. Quack and M. A. Suhm, in *Conceptual Perspectives in Quantum Chemistry*, edited by J.-L. Calais and E. S. Kryachko, *Conceptual Trends in Quantum Chemistry*, Vol. III (Kluwer, Dordrecht, 1997), pp. 417–465.

⁶W. Klopper, M. Quack, and M. Suhm, *J. Chem. Phys.* **108**, 10096 (1998).

⁷M. Quack, in *Femtosecond Chemistry*, edited by J. Manz and L. Woeste, *Proceedings of the Berlin Conference on Femtosecond Chemistry*, Berlin,

March 1993 (Verlag Chemie, Weinheim, 1995), Chap. 27, pp. 781–818.

⁸D. M. Dennison, *Astrophys. J.* **62**, 84 (1925).

⁹I. M. Mills, *Mol. Phys.* **1**, 107 (1958).

¹⁰D. L. Gray and A. G. Robiette, *Mol. Phys.* **37**, 1901 (1979).

¹¹M. Lewerenz and M. Quack, *J. Chem. Phys.* **88**, 5408 (1988).

¹²T. J. Lee, J. M. L. Martin, and P. R. Taylor, *J. Chem. Phys.* **102**, 254 (1995).

¹³R. J. Duchovic, W. L. Hase, H. B. Schlegel, M. J. Frisch, and K. Raghavachari, *Chem. Phys. Lett.* **89**, 120 (1982).

¹⁴R. J. Duchovic, W. L. Hase, and H. B. Schlegel, *J. Phys. Chem.* **88**, 1339 (1984).

¹⁵S. Peyerimhoff, M. Lewerenz, and M. Quack, *Chem. Phys. Lett.* **109**, 563 (1984).

¹⁶F. B. Brown and D. G. Truhlar, *Chem. Phys. Lett.* **113**, 441 (1985).

¹⁷D. M. Hirst, *Chem. Phys. Lett.* **122**, 225 (1985).

¹⁸H. B. Schlegel, *J. Chem. Phys.* **84**, 4530 (1986).

¹⁹M. T. Raynes, P. Lazzarotti, R. Zanasi, A. J. Sadlej, and P. W. Fowler, *Mol. Phys.* **60**, 509 (1987).

²⁰C. Sosa, J. Noga, G. D. Purvis III, and R. J. Bartlett, *Chem. Phys. Lett.* **153**, 139 (1988).

²¹H.-R. Dübal, T.-K. Ha, M. Lewerenz, and M. Quack, *J. Chem. Phys.* **91**, 6698 (1989).

²²R. S. Grev and H. F. Schaefer III, *J. Chem. Phys.* **97**, 8389 (1992).

²³M. S. Gordon and M. W. Schmidt, *J. Am. Chem. Soc.* **115**, 7486 (1993).

²⁴W. Wu and R. McWeeny, *J. Chem. Phys.* **101**, 4826 (1994).

²⁵H. Partridge and C. W. Bauschlicher, Jr., *J. Chem. Phys.* **103**, 10589 (1995).

²⁶M. J. M. Pepper, I. Shavitt, P. v. Ragué Schleyer, M. N. Glukhovtsev, R. Janoschek, and M. Quack, *J. Comput. Chem.* **16**, 207 (1995).

²⁷M. Quack and J. Troe, *Ber. Bunsenges. Phys. Chem.* **78**, 240 (1974).

²⁸M. Quack and J. Troe, *Ber. Bunsenges. Phys. Chem.* **79**, 170 (1975).

²⁹M. Quack, *J. Phys. Chem.* **83**, 150 (1979).

³⁰C. J. Cobos and J. Troe, *Chem. Phys. Lett.* **113**, 419 (1985).

³¹R. J. Duchovic and W. L. Hase, *J. Chem. Phys.* **82**, 3599 (1985).

³²W. L. Hase and R. J. Duchovic, *J. Chem. Phys.* **83**, 3448 (1985).

³³W. L. Hase, S. L. Mondro, R. J. Duchovic, and D. M. Hirst, *J. Am. Chem. Soc.* **109**, 2916 (1987).

³⁴X. Hu and W. L. Hase, *J. Chem. Phys.* **95**, 8073 (1991).

³⁵L. M. Raff, R. Viswanathan, and D. L. Thompson, *J. Chem. Phys.* **80**, 6141 (1984).

³⁶H. Furue, J. F. LeBlanc, P. D. Pacey, and J. M. Whalen, *Chem. Phys.* **154**, 425 (1991).

³⁷C. Iung and C. Leforestier, *J. Chem. Phys.* **90**, 3198 (1989).

³⁸C. Iung and C. Leforestier, *J. Chem. Phys.* **97**, 2481 (1992).

³⁹C. Iung and C. Leforestier, *J. Chem. Phys.* **102**, 8453 (1994).

⁴⁰A. Aboumamd, Dissertation (Dijon), 1984.

⁴¹S. Brodersen and J.-E. Lolck, *J. Mol. Spectrosc.* **126**, 405 (1987).

⁴²L. Halonen, *J. Chem. Phys.* **106**, 831 (1997).

⁴³P. Botschwina, *Chem. Phys.* **68**, 41 (1982).

⁴⁴P. Botschwina, *J. Chem. Soc., Faraday Trans. 2* **84**, 1263 (1988).

⁴⁵V. Špirko and W. P. Kraemer, *J. Mol. Spectrosc.* **133**, 331 (1989).

⁴⁶D. Luckhaus and M. Quack, *Chem. Phys. Lett.* **190**, 581 (1992).

⁴⁷M. Quack, *J. Mol. Struct.* **292**, 171 (1993); **347**, 245 (1995).

⁴⁸A. Beil, D. Luckhaus, and M. Quack, *Ber. Bunsenges. Phys. Chem.* **100**, 1853 (1996).

⁴⁹M. Quack, J. Stohner, and M. A. Suhm, *J. Mol. Struct.* **294**, 33 (1993).

⁵⁰J. M. Hutson, *Annu. Rev. Phys. Chem.* **41**, 123 (1990).

⁵¹M. A. Suhm and D. J. Nesbitt, *Chem. Soc. Rev.* **24**, 45 (1995).

⁵²M. S. Gordon and J. W. Caldwell, *J. Chem. Phys.* **70**, 5503 (1979).

⁵³R. Marquardt and M. Quack (unpublished).

⁵⁴D. Bunker and S. D. Peyerimhoff, *Theor. Chim. Acta* **39**, 217 (1975).

⁵⁵M. Lewerenz, Diploma thesis, Universität Bonn, 1983.

⁵⁶M. Lewerenz, Dissertation, ETH-Zürich, 1987.

⁵⁷S. Peyerimhoff, M. Lewerenz, R. Marquardt, and M. Quack (unpublished).

⁵⁸T. H. Dunning, Jr., *J. Chem. Phys.* **53**, 2823 (1970).

⁵⁹P. Pulay, W. Meyer, and J. E. Boggs, *J. Chem. Phys.* **68**, 5077 (1978).

⁶⁰S. R. Langhoff and E. R. Davidson, *Int. J. Quantum Chem.* **8**, 61 (1974).

⁶¹D. R. Garner and J. B. Anderson, *J. Chem. Phys.* **86**, 4025 (1987).

⁶²J. A. Pople and J. S. Binkley, *Mol. Phys.* **29**, 599 (1975).

⁶³M. W. Chase, Jr., C. A. Davies, J. R. Downey, Jr., D. J. Frurip, R. A. McDonald, and A. N. Syverud, *JANAF Thermochemical Tables*, 3rd ed. (American Chemical Society and American Institute of Physics for the National Bureau of Standards, Woodbury, NY 1985), Vol. 14, Suppl. 1.

- ⁶⁴H. Hollenstein, R. Marquardt, M. Quack, and M. A. Suhm, *J. Chem. Phys.* **101**, 3588 (1994).
- ⁶⁵R. S. Grev, C. L. Janssen, and H. F. Schaefer III, *J. Chem. Phys.* **95**, 5128 (1991).
- ⁶⁶J. Berkowitz, G. B. Ellison, and D. Gutman, *J. Phys. Chem.* **98**, 2744 (1994).
- ⁶⁷C. Yamada, E. Hirota, and K. Kawaguchi, *J. Chem. Phys.* **75**, 5256 (1981).
- ⁶⁸M. Lewerenz, R. Marquardt, and M. Quack, *J. Chem. Soc., Faraday Trans. 2* **84**, 1580 (1988).
- ⁶⁹N. Bjerrum, *Verh. Dtsch. Phys. Ges.* **16**, 737 (1914).
- ⁷⁰P. M. Morse, *Phys. Rev.* **34**, 57 (1929).
- ⁷¹A. Beil, D. Luckhaus, R. Marquardt, and M. Quack, *J. Chem. Soc., Faraday Discuss.* **99**, 49 (1994).
- ⁷²H. Hollenstein, R. R. Marquardt, M. Quack, and M. A. Suhm, *Ber. Bunsenges. Phys. Chem.* **99**, 275 (1995).
- ⁷³R. Signorell, R. Marquardt, M. Quack, and M. A. Suhm, *Mol. Phys.* **89**, 297 (1996).
- ⁷⁴J. M. L. Martin, T. J. Lee, and P. R. Taylor, *J. Chem. Phys.* **97**, 8361 (1992).
- ⁷⁵J. M. L. Martin, P. R. Taylor, and T. J. Lee, *Chem. Phys. Lett.* **205**, 535 (1993).
- ⁷⁶P. Jensen, *J. Mol. Spectrosc.* **133**, 438 (1989).
- ⁷⁷V. Špirko and P. R. Bunker, *J. Mol. Spectrosc.* **95**, 381 (1982).
- ⁷⁸R. J. Wolf, D. S. Bhatia, and W. L. Hase, *Chem. Phys. Lett.* **132**, 493 (1986).
- ⁷⁹A. D. Isaacson, *J. Phys. Chem.* **96**, 531 (1992).
- ⁸⁰H. S. Johnston, *Gas Phase Reaction Rate Theory* (Ronald, New York, 1966).
- ⁸¹E. B. Wilson, Jr., J. C. Decius, and P. C. Cross, *Molecular Vibrations. The Theory of Infrared and Raman Vibrational Spectra* (McGraw-Hill, New York, 1955), Dover ed., New York, 1980.
- ⁸²MAPLE v Release 3 (ETH). Copyright (c) 1981–1994 by Waterloo Maple Software and the University of Waterloo.
- ⁸³J. M. Riveros, *J. Chem. Phys.* **51**, 1269–1270 (1969).
- ⁸⁴J. L. Duncan and I. M. Mills, *Spectrochim. Acta* **20**, 523 (1964).
- ⁸⁵D. W. Marquardt, *J. Soc. Ind. Appl. Math.* **11**, 431–441 (1963).
- ⁸⁶P. Pulay, G. Fogarasi, F. Pang, and J. E. Boggs, *J. Am. Chem. Soc.* **101**, 2550 (1979).
- ⁸⁷E. Hirota and C. Yamada, *J. Mol. Spectrosc.* **96**, 175 (1982).
- ⁸⁸P. R. Bunker, W. P. Kraemer, and V. Špirko, *J. Mol. Spectrosc.* **101**, 180 (1983).
- ⁸⁹P. B. Kelly and S. G. Westre, *Chem. Phys. Lett.* **151**, 253 (1988).
- ⁹⁰J. T. Miller, K. A. Burton, R. B. Weisman, W.-X. Wu, and P. S. Engel, *Chem. Phys. Lett.* **158**, 179 (1989).
- ⁹¹P. R. Bunker, P. Jensen, W. P. Kraemer, and R. Beardsworth, *J. Chem. Phys.* **85**, 3724–3731 (1986).
- ⁹²D. C. Comeau, I. Shavitt, P. Jensen, and P. R. Bunker, *J. Chem. Phys.* **90**, 6491 (1989).
- ⁹³S. G. Lias, J. E. Bartmess, J. F. Liebman, J. L. Holmes, R. D. Levin, and W. G. Mallard, *Gas-Phase Ion and Neutral Thermochemistry* (American Chemical Society and American Institute of Physics for the National Bureau of Standards, Woodbury, NY 1988), Vol. 17, Suppl. 1.
- ⁹⁴O. M. Nefedov, M. P. Egorov, A. I. Ioffe, L. G. Menchikov, P. S. Zuev, V. I. Minkin, B. Y. Simkin, and M. N. Glukhovtsev, *Pure Appl. Chem.* **64**, 265 (1992).
- ⁹⁵J. J. Russell, J. A. Seetula, S. M. Senkan, and D. Gutman, *Int. J. Chem. Kinet.* **20**, 759 (1988).
- ⁹⁶See AIP Document No. PAPS JCPSA6-109-010845 for 27 pages of 3 tables with parameter values for the potential as well as a hardcopy of the FORTRAN source code of the potential METPOT 4. Order by PAPS number in the journal reference from American Institute of Physics, Physics Auxiliary Publication Service, 500 Sunnyside Boulevard, Woodbury, NY 11797-2999. Fax: 516-576-2223, e-mail:paps@aip.org. The price is \$1.50 for each microfiche (98 pages) or \$5.00 for photocopies of up to 30 pages, and \$0.15 for each additional page over 30 pages. Airmail additional. Make checks payable to the American Institute of Physics.
- ⁹⁷A. Bakasov, T. K. Ha, and M. Quack, *J. Chem. Phys.* **109**, 7263 (1998). We have noted that, because of the normalization used in the RCIS program package Gaussian 92/94, the results for parity violating energies E_{pv} calculated by CIS techniques in this paper should be multiplied by 2 in order to be comparable to observable energies. This further amplifies the conclusions concerning the substantial increase of E_{pv} compared to RHF-SDE results.